UNITED NATIONS UNIVERSITY
UNU-GTP
Geothermal Training Programme

Orkustofnun, Grensásvegur 9,
IS-108 Reykjavík, Iceland

Reports 2019
Number 25

MODELLING AN EFFICIENT AND ECONOMICAL GEOTHERMAL POWER PLANT FOR MONTSERRAT

Kenaud E.A. Ryan
Montserrat Utilities, Ltd.
P.O. Box 16, MSR 1110
St. John's
MONTSERRAT W.I.
kenaud.ryan@mul.ms; kenaudryan@yahoo.com

ABSTRACT

Geothermal energy is an environmentally friendly source of renewable heat contained in the earth interior which has been used for heating for centuries and more recently for electricity production. The island of Montserrat lies at the eastern boundary of the Caribbean plate. With an estimated potential of 940 MW from geothermal energy, Montserrat aims to eliminate the current 100% dependency on fossil fuels. The harnessing of geothermal energy in Montserrat began with the exploration and drilling of three geothermal wells, Mon 1, Mon 2, and Mon 3, and has created the avenue for the development of a geothermal power plant.

The objective of this study is to provide information on which the most efficient and economical geothermal power plant for Montserrat by analysing three power plants types: single flash, binary (with cyclopentane as the secondary fluid) and back pressure. The modelling was done in Scilab. Scilab is a numerical computation software that is well suited for this type of power plant modelling. It allows the use of numerous mathematical solutions in combination with numerous combinations of well configurations and boundary conditions. The Scilab software can aid exploring the efficiency and power output of different power plant types.

The results show that binary turbines using cyclopentane as working fluid are preferable. Based on this, recommendations for the development of geothermal energy in Montserrat can be given.

1. INTRODUCTION

As environmental pollution and exploitation of non-renewable energy increases, using renewable energy sources is one of the best options to protect the environment. With this in mind, the island of Montserrat is currently developing renewable sources such as geothermal, solar and wind according to their energy development plan to reduce their dependence on fossil fuels.

The island of Montserrat is located 27 miles southwest of Antigua at 16.45°N and 62.12°W. Montserrat lies within the volcanic arc in the Lesser Antilles (Figure 1) together with other volcanic islands such as Saba, St. Kitts, Nevis, Guadeloupe, Dominica, Martinique, St. Lucia, St. Vincent, the Grenadines and Grenada (DiPippo, 2015).

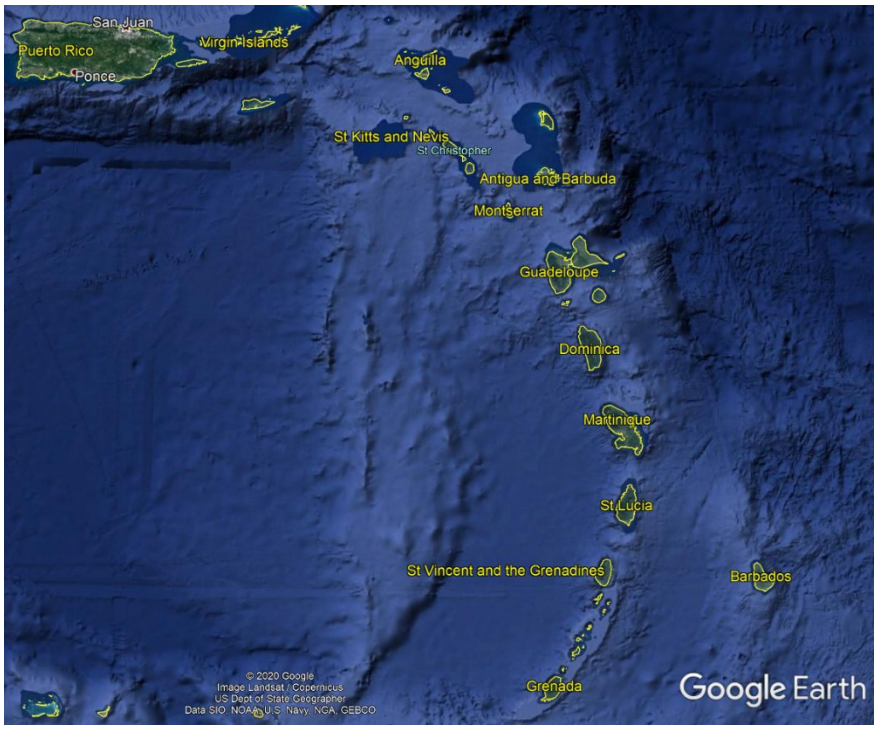

FIGURE 1: Volcanic islands along the eastern boundary of the Caribbean plate (Google Earth, 2019)

Between 1992 and1994, two wind turbines were erected in the St.George's Hill area. In 1995, the Soufriere Hills volcano erupted, leaving the southern part of the island uninhabitable and the wind turbines in the St. George's Hill area unusable. Since then, Montserrat has been again 100% dependent on fossil fuels. In 2019 however, the Government of Montserrat embarked on a solar project and during the first phase of the 1 MW solar project in the Brades area, 250 kW were installed.

The dependency on fossil fuels for electricity generation has been a long-standing burden for the island of Montserrat. With an estimated 940 MW potential of geothermal energy (Battoccletti, 1999), the country has started to exploit the resources with the drilling of three geothermal wells, Mon 1, Mon 2, and Mon 3, all of which are located in the southern part of the island. With this in mind, the Government of Montserrat (GoM) in 2016 stated on their energy development plan until 2030, the goal of achieving 100% renewable energy in the electricity sector by 2020 (MCWL&E, 2016).

In this report, two geothermal wells, Mon 1 and Mon 2, are analysed. The drilling of well Mon 1 started on 17th March, 2013 and ended on 13th May, 2013 at a total depth of 2298 m, with a flow of 20.5 kg/s at a well head pressure of 5 bar-g, an enthalpy of 973.4 kJ/kg, and a temperature of 245°C. The drilling of Mon 2 started on 19th May and ended on 1st October, 2013 at a total depth of 2870 m, with a flow of 13.5 kg/s, a well head pressure of 5 bar-g, an enthalpy of 1021 kJ/kg and a temperature of 250°C (Brophy et al., 2014). Well Mon 3 was drilled in late 2016, but suffered a partial collapse but was reported to have reached temperatures in excess of 230°C. In this report, well Mon 3 is not considered.

Both wells, Mon 1 and Mon 2, were tested and the capacity was estimated to lie between 1.5 and 2.0 MWe (Capuano, 2014). This could be very beneficial for Montserrat, help to reduce the dependency on fossil fuels, and thereby the island's carbon foot print. In 2016, with about 5.4 MW available on-line, the electricity production in Montserrat amounted to 24 GWh (Worldometer, 2019).

In this report, three different types of energy conversion geothermal plants were modelled for wells Mon 1 and Mon 2, i.e., single-flash, binary and back-pressure power plants, to determine the best geothermal plant for the island of Montserrat.

2. LITERATURE REVIEW

2.1 Types of geothermal plants and operation

In geothermal energy utilization, six types of geothermal power plants are currently in use. These are single-flash, double-flash, triple-flash, dry-steam, back-pressure and binary plants (DiPippo, 2015). In this project the focus will be on only three of the six plant types, i.e. single-flash, binary and wellhead geothermal plants, with last one only based on the principles of back-pressure plants. Each type will be analysed in the context of the geothermal field on Montserrat.

2.1.1 Single-flash plant

The single-flash steam plant is known to be the mainstay of the geothermal power industry and is most commonly installed in newly developed liquid-dominated geothermal fields. The single-flash plant is relatively cost effective in terms of land required to support the operation compared to other power plant types. A flash plant needs roughly 1,200 m^2/MW including well pads, pipe routes, the power plant, and substation. For comparison, a coal fire plant needs 40,000 m^2/MW (including the power station plus area to be strip-mined for 30 years) and a solar photovoltaic plant needs 66,000 m^2/MW (power station only) (DiPippo, 2015). Figure 2 shows the layout of a typical single-flash geothermal plant including the main components that are used for operation. These components are also listed in Table 1.

Single-flash power plants are operated as follows: at pressures exceeding atmospheric pressure the geothermal, saturated brine flows through a pipe line with throttle valve from the production well to the separator. From the separator, the saturated vapour is sent to a turbine where a generator produces electricity. The exhaust from the turbine is then condensed in the condenser. The saturated liquid exiting the separator is usually reinjected into an injection well. In the condenser, the vapour is cooled, e.g., by circulating through a cooling tower, with non-condensable gases also being disposed of.

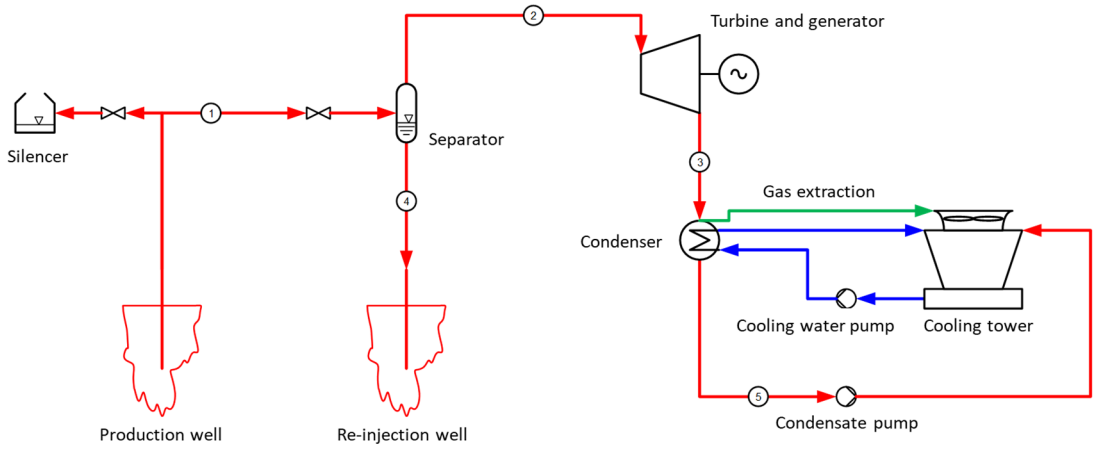

FIGURE 2: The layout of a single-flash power plant

2.1.2 Binary power plants

Similar to conventional fossil or nuclear power plants, the working fluid in a binary cycle power plant undergoes a closed cycle comparable to the organic Rankine power cycle (ORC). These power plants are particularly well suited for modules that produce 1-10 MW of electricity. The geothermal binary power plant utilizes a secondary working fluid, usually hydrocarbons such as propane, isobutene, and isopentane (DiPippo, 1999) or others which have a low boiling point and high vapour pressure at low temperatures in comparison to steam. A binary power plant can be factory built, tested, assembled as skid-mounted units and shipped directly to the site for rapid field installation. Any number of units can be connected to match the power potential of the resource. Binary power plants as shown in Figure 3 are particularly appropriate for low-temperature geothermal resources between 85 and 170°C (Dickson and Fanelli, 2004).

TABLE 1: Major equipment items for geothermal power plants
(DiPippo, 1999)

Equipment	Type of geothermal plant		
	Single flash	**Binary**	**Wellhead**
Steam and/or brine supply:			
Down hole pump	No (poss.)	Yes	No
Wellhead valve and controls	Yes	Yes	Yes
Silencers	Yes	No	Yes
Sand/particulate remover	No	Yes	No
Steam piping	Yes	Yes	Yes
Steam cyclone separator	Yes	No	Yes
Brine piping	Yes	Yes	Yes
Brine booster pumps	Poss.	Poss.	Poss.
Final moisture separator	Yes	No	Yes
Heat exchangers:			
Evaporators	No	Yes	No
Condensers	Yes	Yes	Yes
Turbine-generator and controls:			
Steam turbines	Yes	No	Yes
Organic vapor turbine	No	Yes	No
Control systems	Yes	Yes	Yes
Plant pumps:			
Condensate	Yes	Yes	Yes
Cooling water circulation	Yes	Yes	Yes
Brine re-injection	Yes	Yes	Yes
Non-condensable gas removal system:			
Steam-jet ejectors	Yes	No	Yes
Compressors	Poss.	No	Poss.
Vacuum pumps	Poss.	Poss.	Poss.
Cooling towers:			
Wet type	Yes (No)	Poss	Yes (No)
Dry type	Poss.	Poss.	Poss.
NOTES : Yes = generally used; No = generally not used; Poss. = possibly used under certain circumstances.			

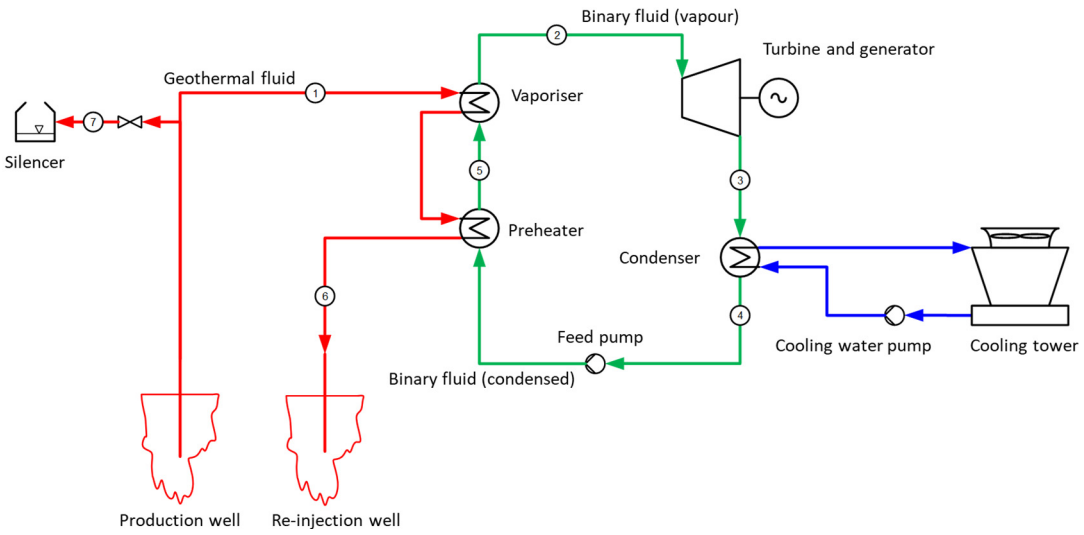

FIGURE 3: The layout of a binary geothermal plant

The layout of a binary plant is shown in Figure 3, the different components are listed in Table 1. In a binary power plant, the geothermal brine is pumped from the production well to the vaporizer where it heats the secondary fluid. The saturated vapour of the secondary fluid enters the turbine and expands, turning the shaft of the generator producing electricity. Then the working fluid exits the turbine and is condensed to a saturated liquid in the condenser. The condensate liquid from the condenser is pumped through the cooling tower. The secondary fluid is pumped back to the preheater where it is re-heated by the geothermal brine and the cycle is repeated. The geothermal fluid from the evaporator and preheater is injected into the reinjection well while the silencer is used as the emergency exhaust (Clark, 2014).

2.1.3 Wellhead (back-pressure) power plants

Wellhead power plant as shown in Figure 4 have been used for decades by the geothermal industry and are very similar to condensing power plants, with the exception of the condenser and a cooling system. (Gudmundsson and Hallgrímsdóttir, 2016). Wellhead units can be connected to wells with an output of up to 10-15 MW. They require shorter steam lines than central power plants which collect steam from several wells. The wellhead plants have a modular construction with the turbo generator modules usually factory assembled on a single sled.

In this report only back-pressure wellhead plants will be considered.

Wellhead power generator units are standardized to ensure easy transportation, easy operation including start and stop, maintenance ability, high efficiency and high reliability. Furthermore, wellhead units possess unique characteristics that make them very attractive for certain applications. These include portability, re-usability, modest capital investment and rapid power production capability (DiPippo, 2015). Because the pressure of the steam exhaust from a back-pressure plant is above atmospheric pressure and the steam is condensed, the entire cold end of the plant is not required. As a result, the cost for the plant is considerably lower than the cost for a conventional condensing power plant. However, the power from the well is not utilized as efficiently as in condensing and ORC power plants (Gudmudsson and Hallgrímsdóttir, 2016).

The wellhead (back-pressure) power plant and its component are shown in Figure 4 and listed in Table 1. The two-phase flow is piped from the production well to a separator where the liquid is separated from the steam. Then, the steam is expanded through the turbine where part of the energy of the steam

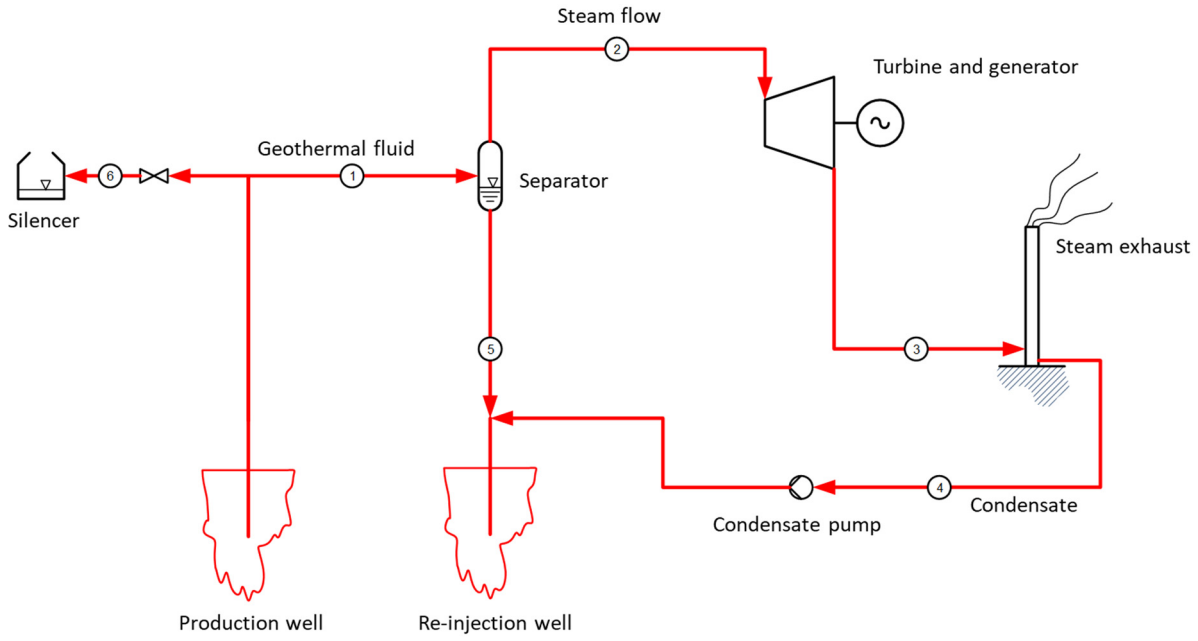

FIGURE 4: Layout of a wellhead (back-pressure) plant

is transformed into mechanical work driving the generator which produces electricity. Leaving the separator, the steam reaches ambient atmospheric pressure when passing the steam exhaust. After leaving the steam exhaust, the condensate is pumped into the reinjection well together with the brine from the separator. The emergency exhaust silencer is used during scheduled maintenance or if problems occur during the operation of the power plant (Gudmundsson and Hallgrímsdóttir, 2016).

3. METHOLOGY

3.1 Data collection

The data used in this report were obtained from the Capuano (2014) report (Tables 2 and 3). The data contain information on the wellhead pressure and mass flow which was collected during long term tests of wells Mon 1 and Mon 2 conducted in 2014. They were inserted into Scilab, a numerical computation software that is particularly well suited for the analysis of energy conversion in geothermal plants. This program allows the use of numerous mathematical solutions in combination with numerous combinations of well configurations and boundary conditions. It was used to create a productivity curve, a decline curve and to calculate the power output of the three different turbine types that are analysed in this project. Input parameters include pressure out of the condenser, enthalpy, entropy and many others which will be discussed later in this report.

TABLE 2: Flow and pressure for well Mon 1

Well head pressure (bar-g)	Total flow rate (kg/s)
3	22.5
4.5	21.5
5.5	19.5
7	17.5
7.5	16.5
7.75	16
8.25	15
8.75	14
9.25	13

TABLE 3: Flow and pressure for well Mon 2

Well head pressure (bar-g)	Total flow rate (kg/s)
1.2	16
2.75	15
3.75	14.5
4.5	14
5.75	12.5
6	12
6.5	11
7	10.5
7.75	9
8.25	7

The power plants were modelled using the Scilab numerical computation software. It assists in analysing the thermodynamics of various fluids in the wells and power plants, outputs are turbine work, separator pressure, and others. The program was setup and run for each of the three types of power plants. Even though many studies to ascertain field characteristics have been conducted, assumptions had to be made for a number of model parameters:

- ✓ Heat exchanger pinch temperature: 5°C;
- ✓ Ambient temperature: 20°C;
- ✓ Condensation temperature in condenser: 45°C;
- ✓ Geothermal fluid mass flow: 20.5 and 13.5 kg/s (to calculate specific power output);
- ✓ Turbine efficiency: 80%;
- ✓ Pump efficiency: 70%;
- ✓ Air cooled condenser parasitic power per MW of condenser heat duty: 11 kW/MW;
- ✓ Wet cooling tower parasitic power per MW of condenser heat duty: 5.7 kW/MW;
- ✓ Binary working fluid: Isopentane, cyclopentane, n-butane, R245fa, n-pentane, propane, R134a.

A productivity curve of the wells is created by assuming that the well pressure loss ($P_{wellhead}$) follows the well flow squared. A decline curve is also estimated for the wells. The flow of a well is then:

$$\dot{m}_{well}(t) = \sqrt{\frac{P_{wellhead} - c(t)}{a(t)}} \quad (1)$$

The parameters *a* and *c* are calculated by assuming a value for the closure pressure (pressure with zero flow) and the maximum flow when the well is producing at atmospheric backpressure. These estimates are based on the report by Capuano (2014).

A simple well decline model is used. It is assumed that the well flow declines exponentially with a time constant of 30 years. The well productivity curve is:

$$\dot{m}_{well}(t) = \sqrt{\frac{P_{wellhead} - c(t)}{a(t)}} \cdot e^{-\frac{Y}{30}} \quad (2)$$

where Y = Years.

The power production models of the power plants were made in Scilab as well. The mathematical foundations and thermodynamic methodology are described in Valdimarsson (2011).

4. RESULTS

4.1 Single-flash plant

Using Scilab, four graphs were produced for Mon 1. Firstly, the productivity curve, secondly, the decline curve, thirdly, the power output vs. well head pressure and fourthly, the power output vs. separator pressure. The results are shown in Figures 5-7 and Table 4 below. All of these graphs were produced in Scilab using Equations 1 and 2 (Petrowiki, 2019).

4.1.1 Well Mon 1

Figure 5 shows the productivity curve for Mon 1. Below a pressure of 3 bar-g, the well flow declines slightly from the estimated curve. Analysing the graph to find the optimal pressure and flow to produce maximum power, a pressure of 4.5 bar-g and a well flow of 21 kg/s was selected.

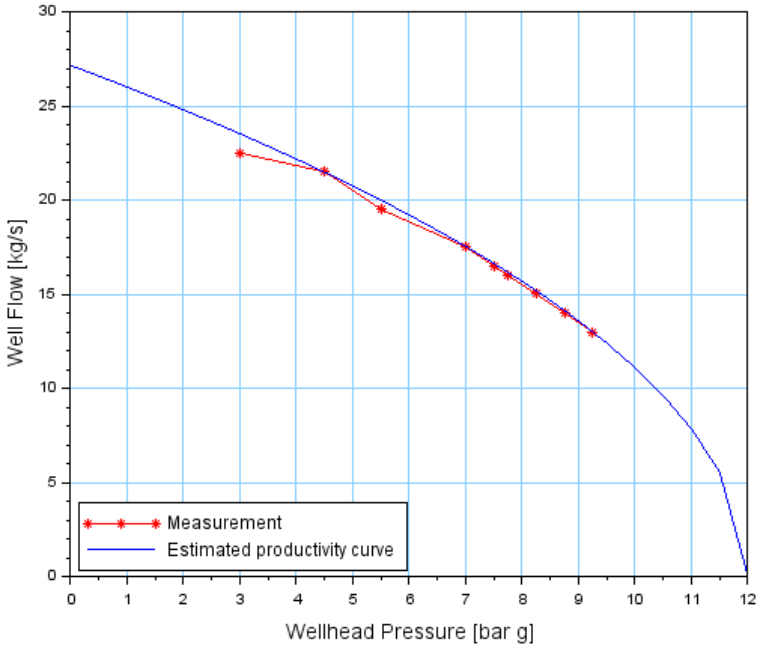

FIGURE 5: Productivity curve for the Mon 1 well

Using the Scilab engineering program, a decline curve was produced with the same data used to produce the productivity curve (Figure 6). As shown in the graph, the pressure and flow were spread over a 30-year period. The use of a 30-year period is supported by DiPippo (2015) who indicates that this is the normal life span of a geothermal well. The term "decline curve analysis" is used to describe

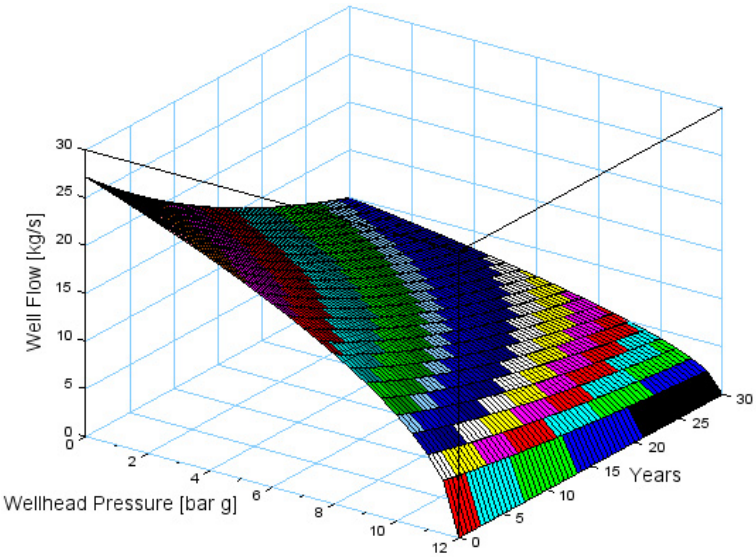

FIGURE 6: Well decline curve for well Mon 1

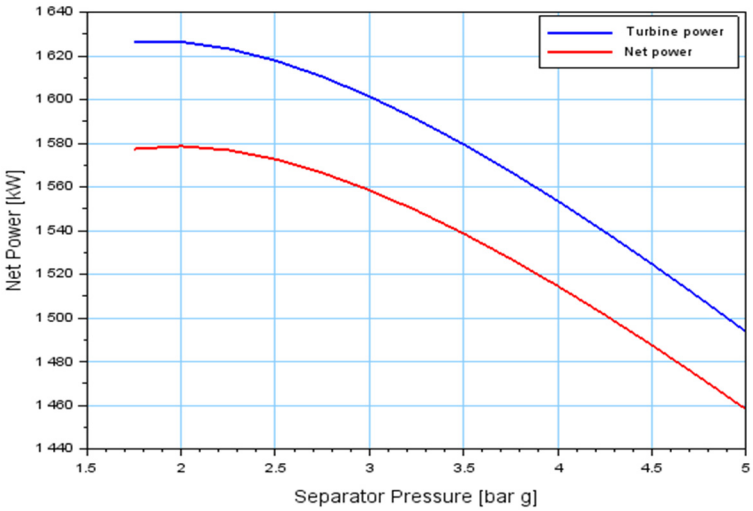

FIGUR 7: Variation of power output with separator pressure for the Mon 1 well for a single-flash power plant

the empirical projection of both flow rate and pressure trends (Sanyal et al, 1989). However, geothermal wells usually decline in productivity harmonically rather than exponentially (Sanyal et al, 2000). The graph shows a gradual decline over the thirty years span.

Using Scilab, a graph showing the separator pressure which will give the optimal power output for well Mon 1 has been generated (Figure 7). Table 4 shows the data collected from the simulation run of the Scilab program. The highlighted row shows the separator pressure which will yield the best output for the well. A wellhead pressure of 5 bar-g and well flow of 20.7 kg/s is assumed. Furthermore, a silica saturation limit for both Mon 1 and Mon 2 at 135°C is considered (Capuano, 2014).

TABLE 4: Simulation data for a single-flash plant using Mon 1 well

Separat. press. (bar-g)	W_dot_net (kW)	W_dot_turbine (kW)	m_dot_steam (kg/s)	m_dot_brine (kg/s)	T_out (°C)
1.75	1577.3	1626.5	4.05	16.69	130.5
2	1578.6	1626.3	3.94	16.79	133.5
2.25	1576.8	1623.3	3.84	16.89	136.2
2.5	1572.6	1617.8	3.75	16.98	138.8
2.75	1566.4	1610.4	3.66	17.07	141.2
3	1558.5	1601.4	3.58	17.15	143.6
3.25	1549.1	1591.0	3.50	17.24	145.8
3.5	1538.6	1579.4	3.42	17.31	147.9
3.75	1527.0	1566.9	3.34	17.39	149.9
4	1514.6	1553.5	3.27	17.46	151.8
4.25	1501.3	1539.4	3.20	17.53	153.6
4.5	1487.5	1524.6	3.13	17.60	155.4
4.75	1473.0	1509.3	3.07	17.66	157.1
5	1458.1	1493.6	3.00	17.73	158.8

4.1.2 Well Mon 2

For well Mon 2 the Scilab program was also used to produce the productivity curve (Figure 8) and decline curve (Figure 9) with the same procedure as stated above.

The graph in Figure 10 shows the power output of the turbine over the separator pressure for Mon 2 well, with Table 5 showing the data collected from the simulation. The highlighted row shows the best separator pressure that would deliver the best power output for well Mon 2.

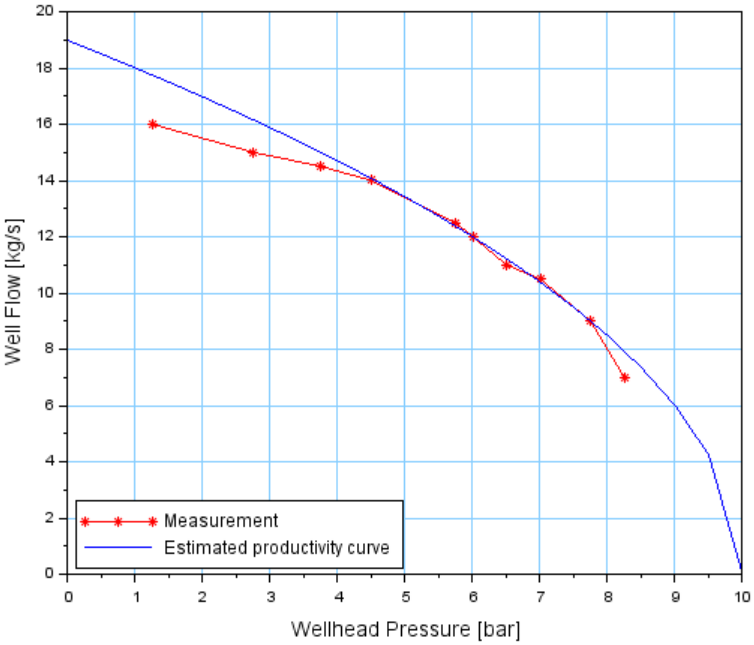

FIGURE 8: Productivity curve for the Mon 2 well

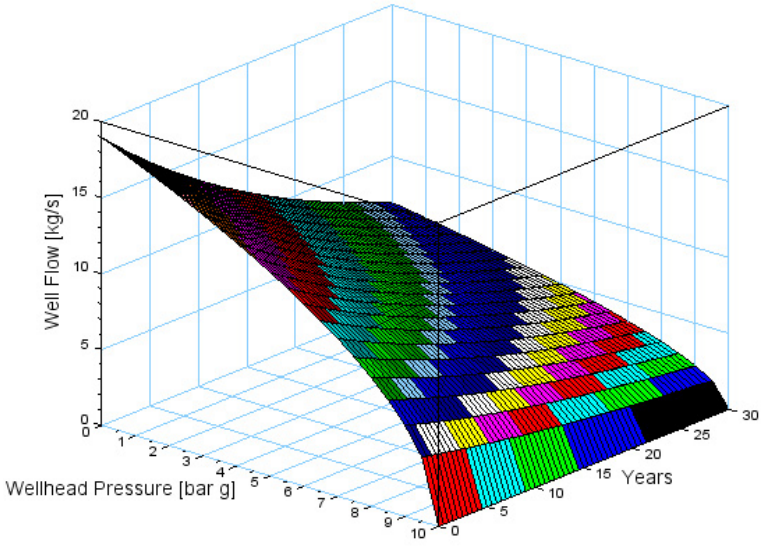

FIGURE 9: Well decline curve for well Mon 2

TABLE 5: Simulation data for a single flash for the Mon 2 well

Separator press. (bar g)	W_dot_net (kW)	W_dot_turbine (kW)	m_dot_steam (kg/s)	m_dot_brine (kg/s)	T_out (°C)
1.75	1135.7	1171.2	2.91	10.50	130.57
2	1140.2	1174.7	2.84	10.56	133.52
2.25	1142.4	1176.1	2.78	10.62	136.27
2.5	1142.9	1175.7	2.72	10.68	138.85
2.75	1141.8	1173.9	2.67	10.74	141.29
3	1139.5	1170.8	2.61	10.79	143.60
3.25	1136.1	1166.8	2.56	10.84	145.80
3.5	1131.8	1161.8	2.51	10.89	147.90
3.75	1126.7	1156.1	2.47	10.94	149.90
4	1120.9	1149.8	2.42	10.99	151.83
4.25	1114.6	1142.8	2.38	11.03	153.67
4.5	1107.8	1135.4	2.33	11.07	155.45
4.75	1100.4	1127.6	2.29	11.12	157.17
5	1092.7	1119.4	2.25	11.16	158.82

4.2 Binary plant

Binary power plants are most effective when the temperature lies between 85 and 170°C (Dickson and Fanelli, 2004). Table 6 below lists selected working fluids commonly used in binary power plants together with their critical temperature, critical pressure and expansion. Four secondary fluids chosen for their high critical temperature are used in the simulation (highlighted in Table 6) to find the optimal power output for each well.

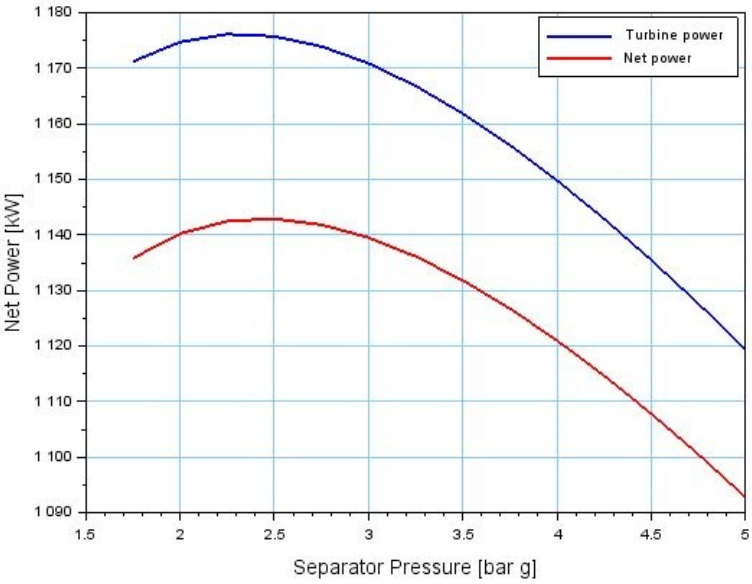

FIGURE 10: Variation of power output with separator pressure for well Mon 2 for a single-flash power plant

TABLE 6: Binary power plant potential working fluids (Clark, 2014)

Name	T_{crit} (ºC)	P_{crit} (MPa)	Expansion
Isopentane	187.2	3.37	Dry
R245fa	154	3.65	Isentropic
n-butane	152	3.79	Dry
Isobutane	135	3.64	Dry
R227ea	102.8	2.99	Dry
R134a	101	4.05	Isentropic
Propane	96.68	4.24	Wet
R236fa	124.9	3.2	Dry
n-pentane	196.5	3.6	Dry
cyclopentane	238.6	4.5	Dry

4.2.1 Well Mon 1

The graphs for the Mon 1 well are shown in Figures 11-14 and the data collected for each graph are shown in Tables 7-10. Figure 15 shows the nose diagram of the different working fluids.

TABLE 7: Mon 1 ORC data with cyclopentane as working fluid

Vaporizer pressure (bar-g)	W_dot_ net (kW)	W_dot_ turbine (kW)	m_dot_ wf (kg/s)	T_out (°C)	Vaporizer pressure (bar-g)	W_dot_ net (kW)	W_dot_ turbine (kW)	m_dot_ wf (kg/s)	T_out (°C)
0.038	22.651	205.09	41.6	50.32	22.4	1855.3	2004.6	18.0	124.0
2.284	1289.5	1463.1	35.7	56.81	24.7	1764.8	1908.8	16.6	131.9
4.530	1722.7	1893.9	32.3	64.03	26.9	1663.8	1801.8	15.3	139.9
6.776	1930.5	2100.2	29.7	71.35	29.2	1553.2	1684.3	14.1	148.1
9.022	2032.7	2200.9	27.5	78.71	31.4	1433.0	1556.2	12.8	156.5
11.26	2073.8	2240.1	25.6	86.11	33.7	1302.4	1416.7	11.5	165.3
13.51	2074.9	2239.0	23.9	93.55	35.9	1159.5	1263.5	10.1	174.6
15.76	2047.7	2209.0	22.3	101.0	38.2	999.86	1091.7	8.72	184.7
18.00	1999.2	2157.2	20.8	108.6	40.4	813.74	890.40	7.08	196.1
20.25	1934.1	2088.1	19.3	116.2	42.7	578.80	634.76	5.03	210.3

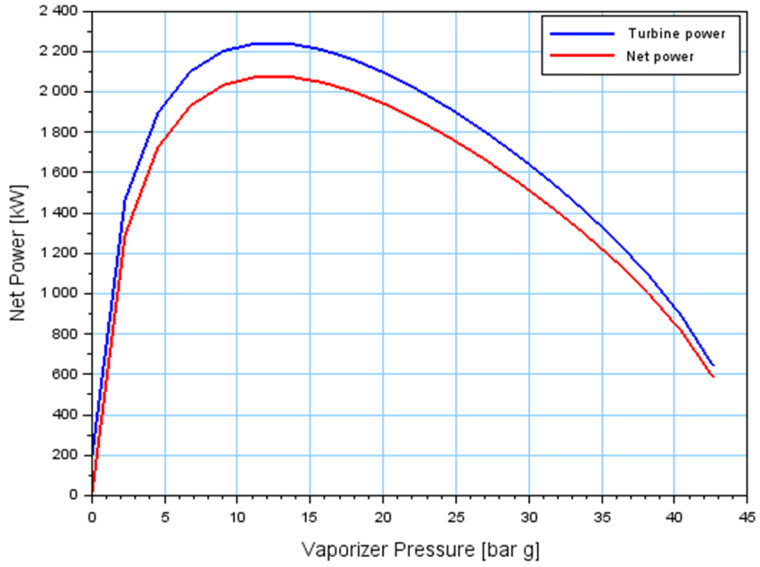

FIGURE 11: Mon 1 well, variation of power output vs. vaporizer pressure f for an ORC plant with cyclopentane as working fluid

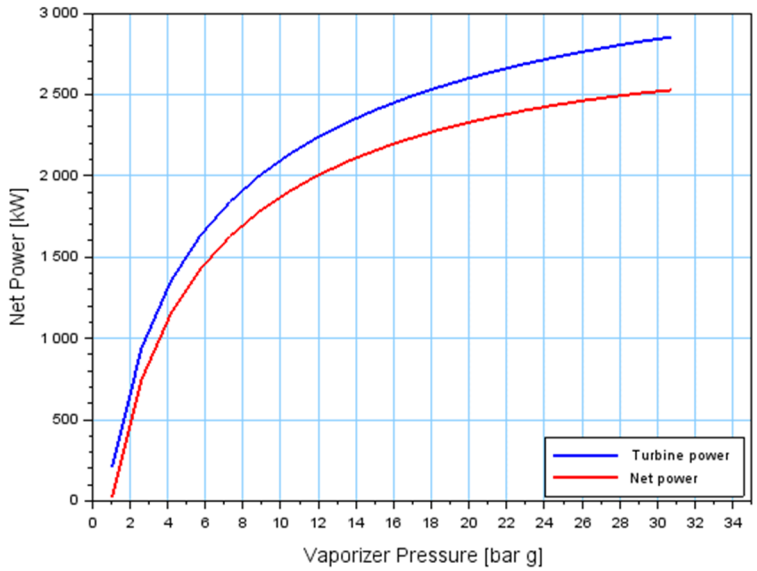

FIGURE 12: Mon 1 well, variation of power output vs. vaporizer pressure for an ORC plant with isopentane as the working fluid

TABLE 8: Mon 1 ORC data with working fluid isopentane

Vaporizer pressure (bar-g)	W_dot_ net (kW)	W_dot_ turbine (kW)	m_dot_ wf (kg/s)	T_out (°C)	Vaporizer pressure (bar-g)	W_dot_ net (kW)	W_dot_ turbine (kW)	m_dot_ wf (kg/s)	T_out (°C)
1.055	20.537	206.54	49.5	48.0	16.69	2222.7	2479.1	35.2	45.6
2.619	748.18	941.02	45.9	45.0	18.26	2276.5	2540.2	34.7	45.7
4.184	1155.9	1354.8	43.2	45.1	19.82	2323.5	2594.6	34.3	45.7
5.748	1428.3	1634.0	41.3	45.2	21.39	2364.9	2643.5	34.0	45.8
7.312	1627.3	1840.1	39.9	45.2	22.95	2401.5	2687.5	33.8	45.8
8.877	1780.8	2000.7	38.7	45.3	24.52	2433.8	2727.5	33.5	45.9
10.44	1903.5	2130.7	37.8	45.3	26.08	2462.3	2763.8	33.4	46.0
12.00	2004.4	2238.9	36.9	45.4	27.65	2487.3	2796.8	33.3	46.0
13.57	2088.9	2330.7	36.3	45.5	29.21	2509.1	2826.7	33.2	46.1
15.13	2160.8	2409.9	35.7	45.5	30.78	2527.5	2853.8	33.2	46.2

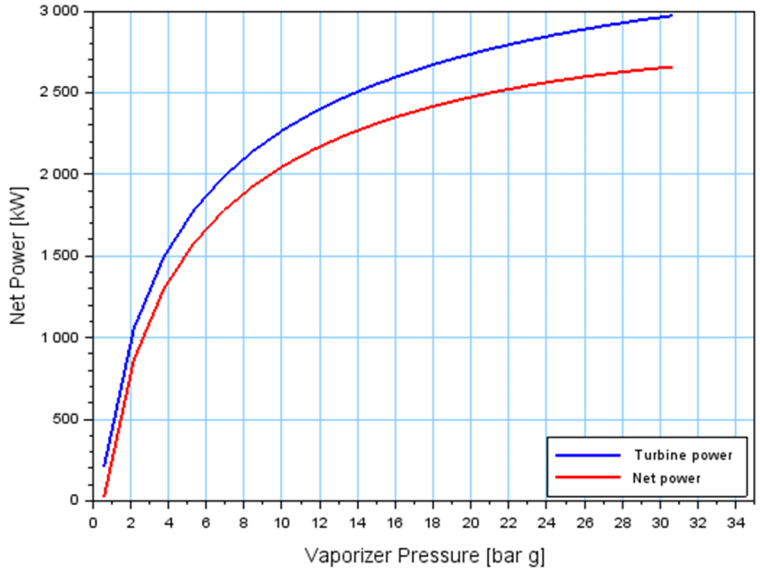

FIGURE 13: Mon 1 well, variation of power output vs. vaporizer pressure for an ORC plant with n-pentane as working fluid

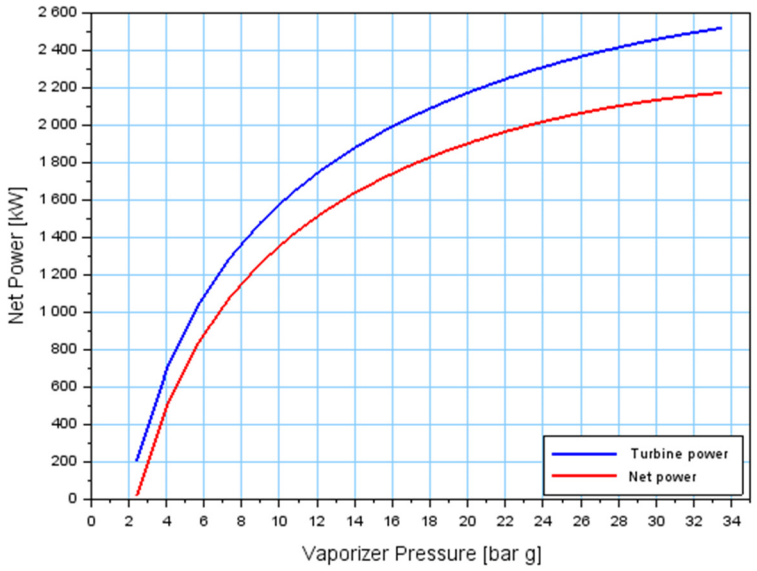

FIGURE 14: Mon 1 well, variation of power output vs. vaporizer pressure for an ORC plant with R245fa as working fluid

TABLE 9: Mon 1 ORC data with working fluid n-pentane

Vaporizer pressure (bar-g)	W_dot_ net (kW)	W_dot_ turbine (kW)	m_dot_ wf (kg/s)	T_out (°C)	Vaporizer pressure (bar-g)	W_dot_ net (kW)	W_dot_ turbine (kW)	m_dot_ wf (kg/s)	T_out (°C)
0.592	20.908	206.01	46.6	48.4	16.4	2365.2	2613.3	32.7	45.6
2.177	865.68	1055.8	42.8	45.0	18.0	2417.4	2672.4	32.3	45.6
3.761	1299.1	1494.4	40.2	45.1	19.6	2463.0	2724.9	32.0	45.7
5.346	1578.7	1780.0	38.4	45.1	21.1	2503.0	2771.9	31.7	45.7
6.930	1779.1	1986.8	37.0	45.2	22.7	2538.3	2814.2	31.5	45.8
8.515	1931.9	2146.1	35.9	45.3	24.3	2569.3	2852.5	31.3	45.9
10.10	2053.2	2274.1	35.0	45.3	25.9	2596.7	2887.1	31.1	45.9
11.68	2152.2	2379.9	34.3	45.4	27.5	2620.5	2918.5	31.1	46.0
13.26	2234.9	2469.4	33.7	45.4	29.1	2641.2	2946.9	31.0	46.0
14.85	2305.0	2546.3	33.2	45.5	30.7	2658.5	2972.4	31.0	46.1

TABLE 10: Mon 1 ORC data with working fluid R245fa

Vaporizer pressure (bar-g)	W_dot_ net (kW)	W_dot_ turbine (kW)	m_dot_ wf (kg/s)	T_out (°C)	Vaporizer pressure (bar-g)	W_dot_ net (kW)	W_dot_ turbine (kW)	m_dot_ wf (kg/s)	T_out (°C)
2.442	20.557	208.10	91.6	47.6	18.79	1857.4	2121.9	75.0	45.6
4.077	512.81	708.57	88.3	45.0	20.42	1914.7	2187.4	74.5	45.7
5.712	838.14	1040.6	85.1	45.1	22.06	1964.9	2245.9	74.1	45.8
7.347	1075.4	1285.1	82.7	45.2	23.69	2009.1	2298.5	73.9	45.8
8.982	1258.8	1476.0	80.9	45.2	25.33	2047.8	2345.9	73.7	45.9
10.61	1406.0	1630.8	79.4	45.3	26.96	2081.5	2388.4	73.6	46.0
12.25	1527.5	1760.0	78.1	45.4	28.60	2110.5	2426.6	73.7	46.0
13.88	1629.6	1870.0	77.1	45.4	30.23	2135.1	2460.5	73.8	46.1
15.52	1716.8	1965.1	76.3	45.5	31.87	2155.3	2490.4	74.1	46.2
17.15	1792.0	2048.3	75.6	45.6	33.51	2170.9	2516.2	74.4	46.2

All the tested working fluids except for cyclopentane, display the same behaviour. The calculated work output is very high and the calculated return temperature low. This is caused by a low critical temperature of the working fluid relative to the source fluid temperature.

The heat input to an ORC cycle is limited by the hot side pinch, which is the lowest temperature difference between the source fluid and the working fluid at any location in the hot side of the plant. If the pinch is zero, then no more heat can be transferred from the source fluid to the working fluid. Normally this pinch point is at the bubble point, the point in the hot side heat exchanger train where the working fluid reaches liquid saturation and the first vapour bubble is created, therefore the name “bubble point”. This is the common design practise for saturated vapour ORC plants today.

If the working fluid’s critical temperature is too low, this pinch point will move from the bubble point to the inflow of the liquid working fluid into the first preheater in the hot side heat exchanger train. Obviously, the source fluid temperature is then almost equal to the (low) temperature of the liquid working fluid coming from the condenser (or the recuperator, if installed). This will cause scaling risk and controllability issues. Therefore, fluids with a critical temperature much lower than the source fluid inflow temperature are not feasible. No binary plant vendor is known to have solved the controllability issues which may arise for having this location of the pinch point. The hot side pinch of the cycle is not located at the bubble point but at the inflow of the cold liquid working fluid into the preheater for all tested working fluids except cyclopentane. Therefore, it can be concluded that the only possible working fluid for an ORC plant for well Mon 1 is cyclopentane.

This can also be seen in the so-called nose diagram, which is shown in Figure 15. In the nose diagram the return temperature is plotted over the net power plant power, and the “nosetip” shows the best value combination of power and return temperature. All the working fluids with a low critical temperature relative to the source temperature fall on the same curve.

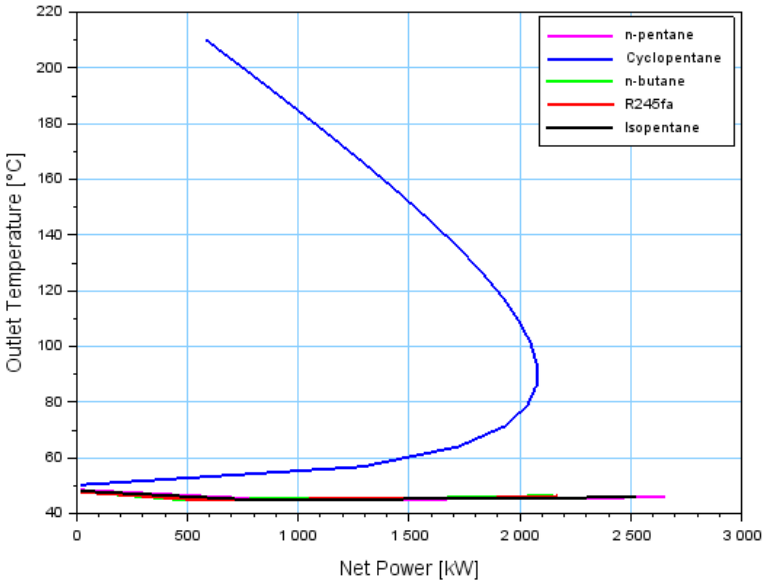

FIGURE 15: Nose diagram of secondary fluids used in the simulation for Mon 1

4.2.2 Well Mon 2

For the Mon 2 well, graphs are shown in Figures 16-19 and data collected for each graph are listed in Tables 11-14. Figure 20 shows the nose diagram for different working fluids of which four were used in the simulations as shown in Table 6.

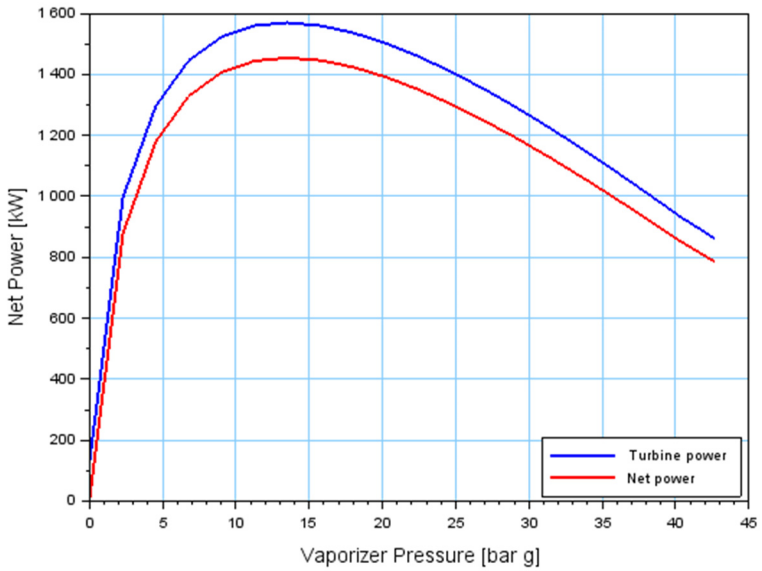

FIGURE 16: Mon 2 well, variation of power output vs. vaporizer pressure for an ORC plant with cyclopentane as working fluid

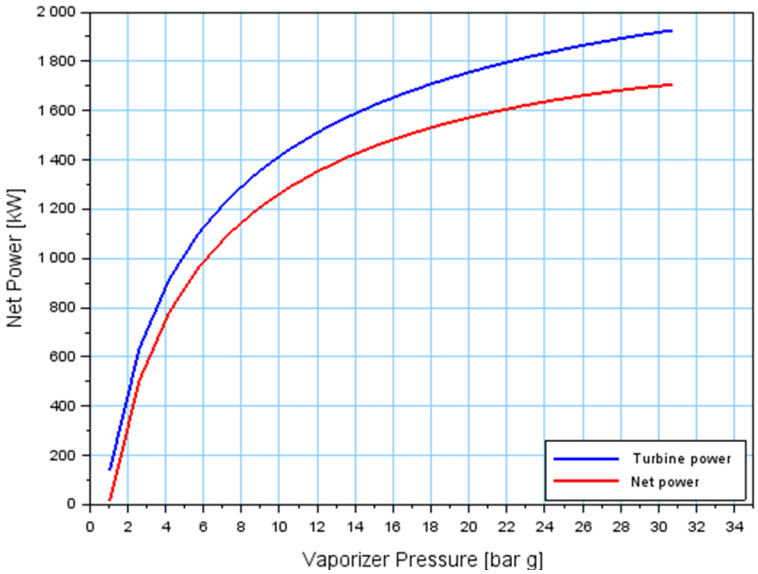

FIGURE 17: Mon 2 well, variation of power output vs. vaporizer pressure for an ORC plant with isopentane as working fluid

All the tested working fluids except cyclopentane display the same behaviour for well Mon 2, just as they did for well Mon 1. The calculated work output is very high and the calculated return temperature low. This is caused by a low critical temperature of the working fluid relative to the source fluid temperature. Therefore, it can be concluded that the only possible working fluid for an ORC plant for well Mon 2 is cyclopentane. This is also seen on the so-called nose diagram, which is shown in Figure 20. All the working fluids with a low critical temperature relative to the source temperature fall on the same curve.

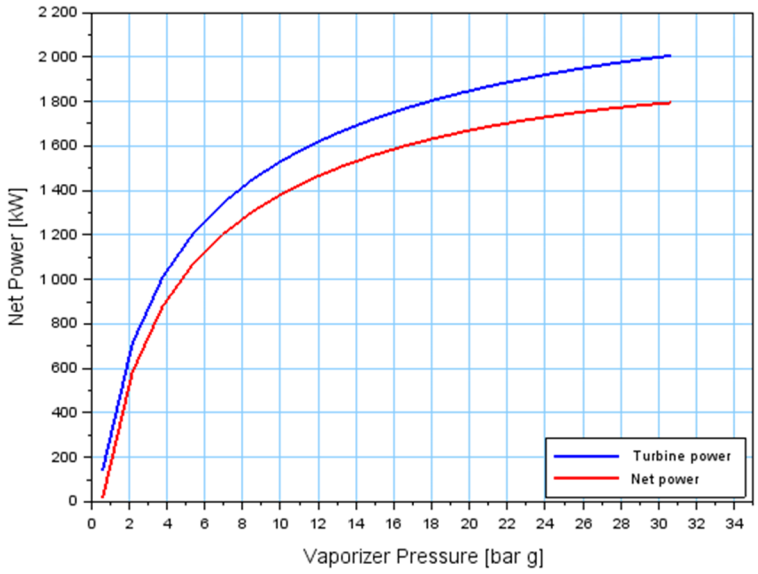

FIGURE 18: Mon 2 well, variation of power output vs. vaporizer pressure for an ORC plant with n-pentane as working fluid

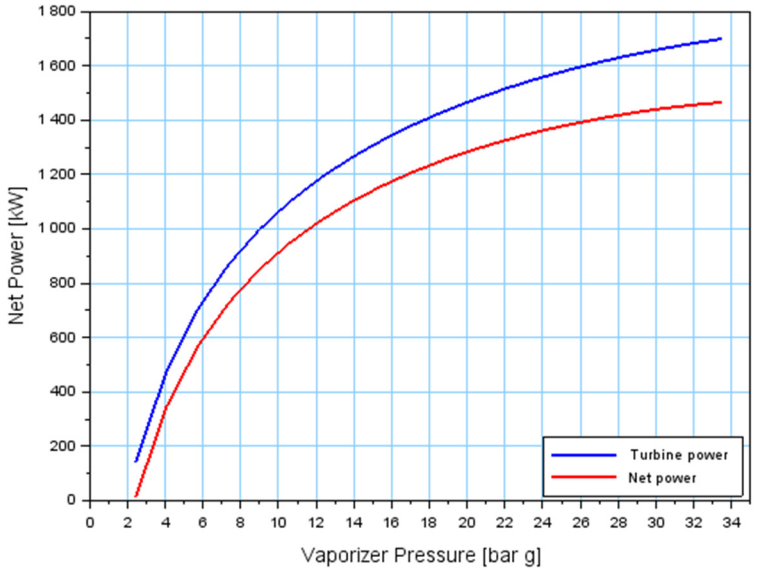

FIGURE 19: Mon 2 well, variation of power output vs. vaporizer pressure for an ORC plant with R245fa as working fluid

TABLE 11: Mon 2 well, ORC data with working fluid cyclopentane

Vaporizer pressure (bar-g)	W_dot_net (kW)	W_dot_turbine (kW)	m_dot_wf (kg/s)	T_out (°C)	Vaporizer pressure (bar-g)	W_dot_net (kW)	W_dot_turbine (kW)	m_dot_wf (kg/s)	T_out (°C)
0.038	15.309	138.61	28.1	50.19	22.49	1349.3	1457.9	13.1	116.4
2.284	877.54	995.70	24.3	55.52	24.74	1301.0	1407.1	12.3	123.4
4.530	1179.0	1296.1	22.1	61.93	26.99	1246.9	1350.3	11.5	130.4
6.776	1328.4	1445.1	20.4	68.55	29.23	1188.2	1288.4	10.7	137.4
9.022	1406.7	1523.0	19.0	75.26	31.48	1125.5	1222.3	10.0	144.5
11.26	1443.8	1559.6	17.8	82.01	33.72	1059.5	1152.5	9.37	151.6
13.51	1454.2	1569.2	16.7	88.81	35.97	990.80	1079.7	8.69	158.6
15.76	1445.9	1559.8	15.7	95.65	38.22	920.09	1004.6	8.02	165.7
18.00	1423.6	1536.1	14.8	102.5	40.46	848.76	928.71	7.38	172.6
20.25	1390.7	1501.4	13.9	109.4	42.71	784.76	860.62	6.82	178.7

TABLE 12: Mon 2 well, ORC data with working fluid isopentane

Vaporizer pressure (bar-g)	W_dot_ net (kW)	W_dot_ turbine (kW)	m_dot_ wf (kg/s)	T_out (°C)	Vaporizer pressure (bar-g)	W_dot_ net (kW)	W_dot_ turbine (kW)	m_dot_ wf (kg/s)	T_out (°C)
1.055	13.880	139.59	33.4	47.9	16.69	1500.4	1673.5	23.7	45.6
2.619	505.02	635.19	31.0	45.0	18.26	1536.7	1714.8	23.4	45.7
4.184	780.29	914.55	29.2	45.1	19.82	1568.5	1751.5	23.2	45.7
5.748	964.18	1103.0	27.9	45.2	21.39	1596.5	1784.5	23.0	45.8
7.312	1098.5	1242.1	26.9	45.2	22.95	1621.2	1814.3	22.8	45.8
8.877	1202.0	1350.5	26.1	45.3	24.52	1643.0	1841.2	22.6	45.9
10.44	1284.9	1438.3	25.5	45.3	26.08	1662.2	1865.8	22.5	46.0
12.00	1353.0	1511.3	24.9	45.4	27.65	1679.1	1888.1	22.4	46.0
13.57	1410.1	1573.3	24.5	45.5	29.21	1693.8	1908.3	22.4	46.1
15.13	1458.6	1626.8	24.1	45.5	30.78	1706.3	1926.6	22.4	46.2

TABLE 13: Mon 2 well, ORC data with working fluid n-pentane

Vaporizer pressure (bar-g)	W_dot_ net (kW)	W_dot_ turbine (kW)	m_dot_ wf (kg/s)	T_out (°C)	Vaporizer pressure (bar-g)	W_dot_ net (kW)	W_dot_ turbine (kW)	m_dot_ wf (kg/s)	T_out (°C)
0.592	14.131	139.23	31.5	48.2	16.43	1596.6	1764.1	22.1	45.6
2.177	584.34	712.73	28.9	45.0	18.02	1631.9	1804.0	21.8	45.6
3.761	876.97	1008.7	27.1	45.1	19.60	1662.7	1839.5	21.6	45.7
5.346	1065.6	1201.5	25.9	45.1	21.19	1689.7	1871.2	21.4	45.7
6.930	1200.9	1341.1	25.0	45.2	22.77	1713.5	1899.8	21.2	45.8
8.515	1304.0	1448.7	24.2	45.3	24.36	1734.5	1925.6	21.1	45.9
10.10	1385.9	1535.1	23.6	45.3	25.94	1752.9	1949.0	21.0	45.9
11.68	1452.8	1606.5	23.1	45.4	27.53	1769.1	1970.2	20.9	46.0
13.26	1508.6	1666.9	22.7	45.4	29.11	1783.0	1989.4	20.9	46.0
14.85	1556.0	1718.9	22.4	45.5	30.70	1794.7	2006.6	20.9	46.1

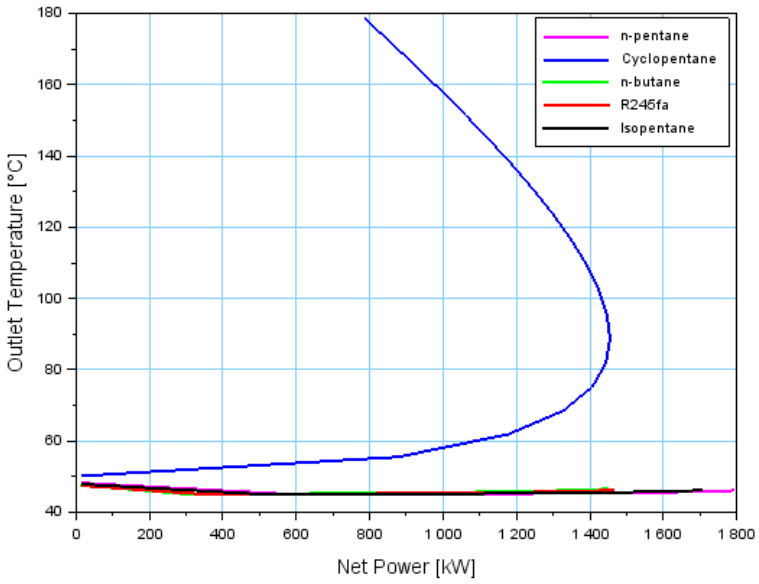

FIGURE 20: Nose diagram of five different secondary fluids used in the simulation for well Mon 2

TABLE 14: Mon 2 well, ORC data with working fluid R245fa

Vaporizer pressure (bar-g)	W_dot_ net (kW)	W_dot_ turbine (kW)	m_dot_ wf (kg/s)	T_out (°C)	Vaporizer pressure (bar-g)	W_dot_ net (kW)	W_dot_ turbine (kW)	m_dot_ wf (kg/s)	T_out (°C)
2.442	13.894	140.65	61.9	47.4	18.7	1253.9	1432.4	50.6	45.6
4.077	346.15	478.29	59.6	45.0	20.4	1292.5	1476.6	50.3	45.7
5.712	565.76	702.43	57.4	45.1	22.0	1326.5	1516.1	50.0	45.8
7.347	725.94	867.49	55.8	45.2	23.6	1356.3	1551.7	49.9	45.8
8.982	849.74	996.33	54.6	45.2	25.3	1382.4	1583.6	49.7	45.9
10.61	949.14	1100.8	53.6	45.3	26.9	1405.1	1612.4	49.7	46.0
12.25	1031.1	1188.1	52.7	45.4	28.6	1424.8	1638.1	49.7	46.0
13.88	1100.0	1262.3	52.0	45.4	30.2	1441.4	1661.1	49.8	46.1
15.52	1158.9	1326.5	51.5	45.5	31.8	1455.0	1681.3	50.0	46.2
17.15	1209.7	1382.7	51.0	45.6	33.5	1465.6	1698.7	50.2	46.2

4.3 Single-flash with a binary bottoming plant

The layout of a bottoming plant (Figure 21) was originally not a part of this project. It was added due to the fact that a binary plant does not work well with temperatures above 185°C. The two wells analysed in this project have temperatures of 245 and 250°C, respectively. So, using the fluid from the separator for the single-flash plant, simulations were run for both wells to model the possible power output. Five secondary fluids, that is propane, R236fa, R246fa, isobutane and R134a, were used. The results are shown in Figure 22 for Mon 1 and Figure 23 for Mon 2.

The bottoming plant could be beneficial for the overall capacity of the power plant but was abandoned after it was discovered in the Capuano (2014) report that the silica saturation limit for both Mon 1 and Mon 2 is 135°C. As shown in Figures 22 and 23, the average temperature out is between 60 and 90°C. These low temperatures would cause scaling in the reinjection well and pipe lines. It is assumed that the

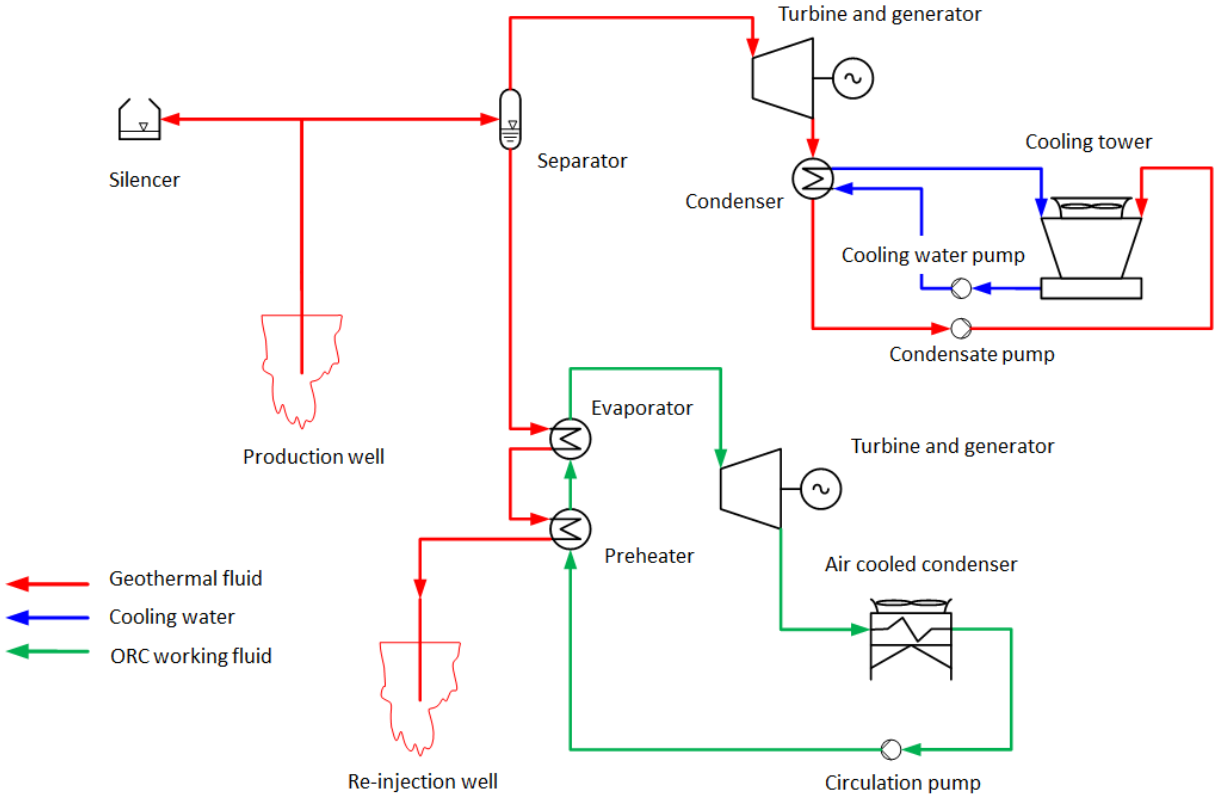

FIGURE 21: A single-flash plant with a bottoming ORC plant

single-flash plant is running at a wellhead pressure of 5 bar-g as described in Sections 4.1.1 for well Mon 1 and 4.1.2 for well Mon 2. The single-flash plant data (Table 15) is as follows:

TABLE 15: Single-flash plant data

Well	Separator pressure (bar-g)	W_dot_net (kW)	W_dot_turbine (kW)	m_dot_brine (kg/s)	T_out (°C)
Mon 1	2.25	1576.8	1623.3	16.89	136.2
Mon 2	2.5	1142.9	1175.7	10.68	138.5

4.3.1 Well Mon 1

The nose diagram for an ORC bottoming plant for well Mon 1 is shown in Figure 22. The return temperature is plotted over the net power plant power, and the "nosetip" shows the best value combination of power and return temperature. The best fluid is refrigerant R236fa with 75°C re-injection temperature and 310 kW net power from the ORC bottoming plant. The fluids R134a and propane do not show any nosetip and are not usable, see Sections 4.2.1 and 4.2.2.

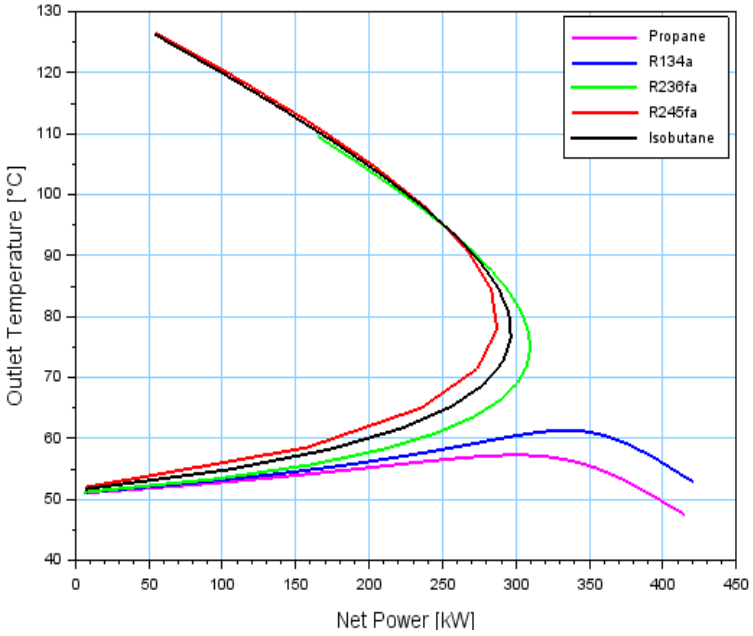

FIGURE 22: Well Mon 1, nose diagram for an ORC bottoming plant

This bottoming plant is not very feasible because of low re-injection temperature which is well below the scaling limit and because of low power output. An ORC plant is complicated and the economics of scale work against such small plants. The smaller the plant, the more expensive it becomes for each kW produced because the price of the individual components is not reduced in the same scale as the plant size, and fixed costs such as design and engineering costs do not scale at all.

4.3.2 Well Mon 2

The nose diagram for an ORC bottoming plant for well Mon 2 is shown in Figure 23. The best fluid is refrigerant R236fa with 74°C re-injection temperature and 228 kW net power from the ORC bottoming plant. Again, the fluids R134a and propane do not show any nosetip and are not usable (Sections 4.2.1 and

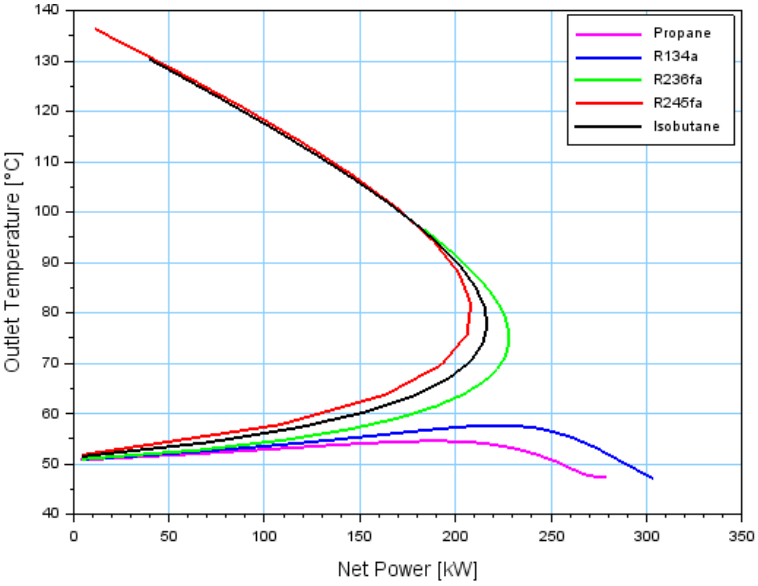

FIGURE 23: Well Mon 2, nose diagram for an ORC bottoming plant

4.2.2). And as mentioned above for Mon 1, the bottoming plant is not feasible because of low re-injection temperature, well below the scaling limit as well as low power output.

4.4 Back-pressure plant

The back-pressure plant is a single-flash plant without a condenser. The turbine exhaust steam is disposed of in a stack into the atmosphere. The turbine's back pressure will be at least equal to the atmospheric pressure. The back-pressure plant has low power output because of the high turbine exhaust pressure but it is a simple plant with low investment cost. The internal plant power consumption is close to zero, as no power is needed for a cooling tower or cooling water pumps. A schematic of a back-pressure plant is shown in Figure 24.

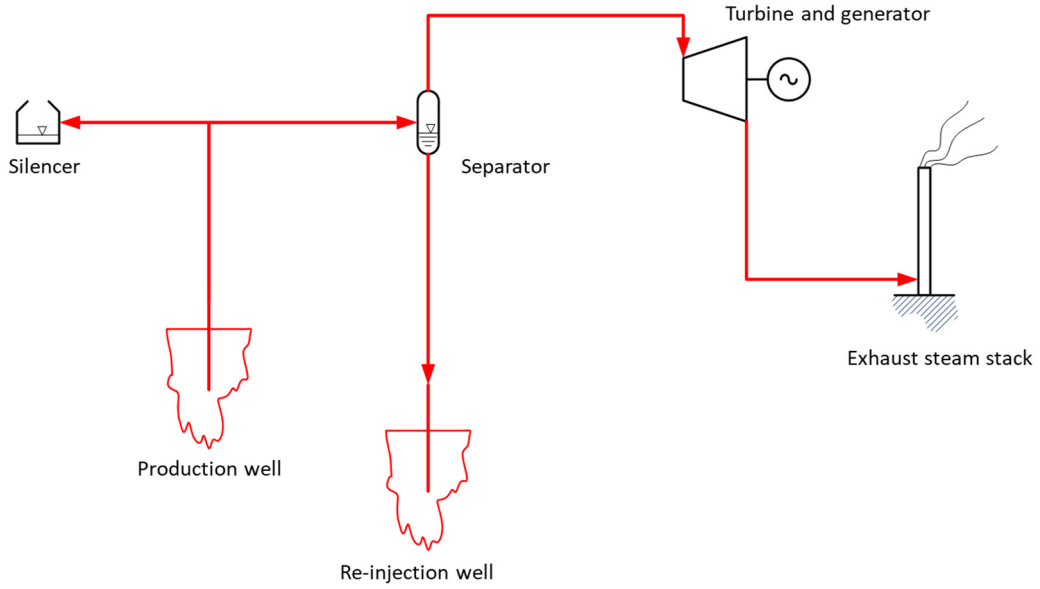

FIGURE 24: Process flow diagram for a back-pressure plant

4.4.1 Mon 1

The graphs in Figure 25 below show the power output of the turbine for different separator pressures (for data, see Table 16). The data were collected by running the simulation in the Scilab program for a back-pressure plant for well Mon 1.

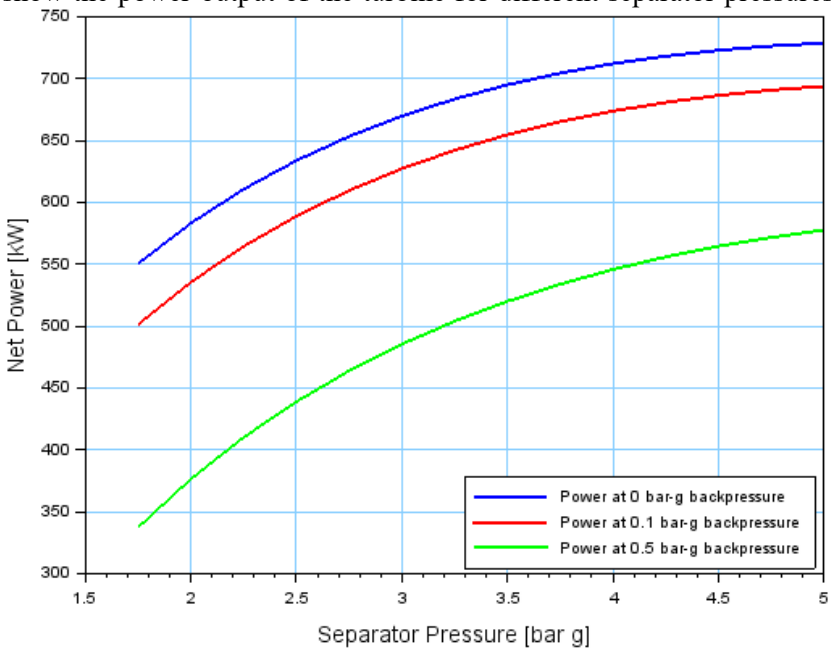

FIGURE 25: Variation of power output vs. separator pressure for well Mon 1, for a back-pressure plant

TABLE 16: Data collected from simulation for a Mon 1 back-pressure plant

Separator pressure (bar-g)	P_bp 0.0 bar-g W_dot (kW)	P_bp 0.1 bar-g W_dot (kW)	P_bp 0.5 bar-g W_dot (kW)	m_dot_ steam (kg/s)	m_dot _brine (kg/s)	T_out (°C)
1.75	550.5	501.4	337.3	4.05	16.69	130.5
2	583.2	535.6	376.5	3.94	16.79	133.5
2.25	610.6	564.4	410.1	3.84	16.89	136.2
2.5	633.8	588.9	439.0	3.75	16.98	138.8
2.75	653.3	609.7	463.9	3.66	17.07	141.2
3	669.8	627.3	485.4	3.58	17.15	143.6
3.25	683.5	642.2	504.0	3.50	17.24	145.8
3.5	695.0	654.7	520.1	3.42	17.31	147.9
3.75	704.5	665.1	533.9	3.34	17.39	149.9
4	712.1	673.8	545.8	3.27	17.46	151.8
4.25	718.2	680.8	555.9	3.20	17.53	153.6
4.5	722.9	686.4	564.5	3.13	17.60	155.4
4.75	726.4	690.7	571.7	3.07	17.66	157.1
5	728.7	693.9	577.6	3.00	17.73	158.8

The best separator pressure is the highest possible pressure, and here a separator pressure of 5 bar-g is assumed. The turbine exhaust flow temperature and enthalpy are calculated as follows:

- ✓ Backpressure 0 bar-g: T = 100.0°C; h = 2513.9 kJ/kg.
- ✓ Backpressure 0.1 bar-g: T = 102.6°C; h = 2525.5 kJ/kg.
- ✓ Backpressure 0.5 bar-g: T = 111.6°C; h = 2564.2 kJ/kg.

4.4.2 Mon 2

The graphs in Figure 26 below show the power output of the turbine for different separator pressures (for data see Table 17). The data were collected by running the simulation in the Scilab program for a back-pressure plant for well Mon 2.

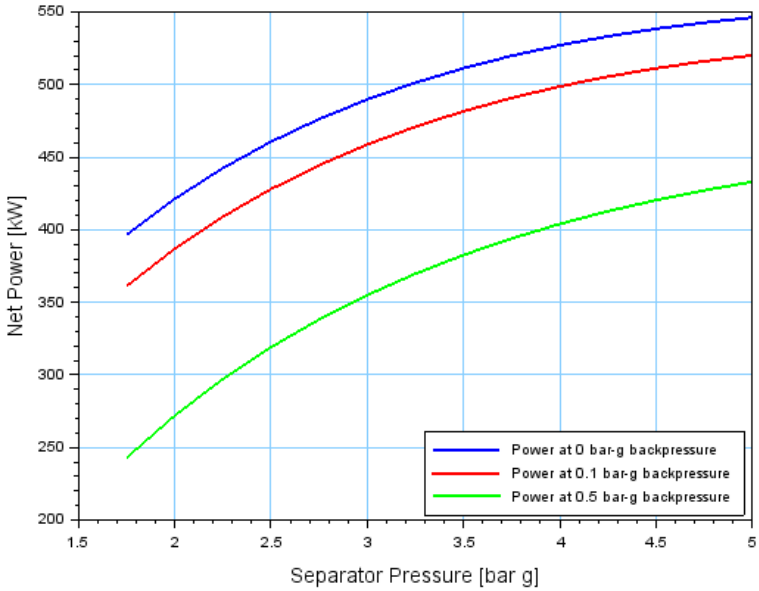

FIGURE 26: Variation of power output vs. separator pressure for well Mon 2, for a back-pressure plant

TABLE 17: Data collected from simulation for a Mon 2 back-pressure plant

Separator pressure (bar-g)	P_bp 0.0 bar-g W_dot (kW)	P_bp 0.1 bar-g W_dot (kW)	P_bp 0.5 bar-g W_dot (kW)	m_dot_ steam (kg/s)	m_dot_ brine (kg/s)	T_out (°C)
1.75	396.4	361.0	242.9	2.91	10.50	130.5
2	421.2	386.8	271.9	2.84	10.56	133.5
2.25	442.4	408.9	297.1	2.78	10.62	136.2
2.5	460.6	428.0	319.0	2.72	10.68	138.8
2.75	476.2	444.4	338.1	2.67	10.74	141.2
3	489.7	458.6	354.9	2.61	10.79	143.6
3.25	501.3	470.9	369.6	2.56	10.84	145.8
3.5	511.2	481.6	382.6	2.51	10.89	147.9
3.75	519.8	490.8	393.9	2.47	10.94	149.9
4	527.1	498.7	403.9	2.42	10.99	151.8
4.25	533.2	505.4	412.7	2.38	11.03	153.6
4.5	538.4	511.2	420.4	2.33	11.07	155.4
4.75	542.7	516.0	427.1	2.29	11.12	157.1
5	546.1	520.0	432.9	2.25	11.16	158.8

The turbine exhaust flow temperature and enthalpy for 5 bar-g separator pressure was calculated with the same values as for well Mon 1.

4.5 Back-pressure plant with a binary bottoming plant

As mentioned before, the bottoming plant was not an original part of this project. The layout of the plant combining this with the back-pressure plant is shown in Figure 27. The vaporizer and preheater of the ORC plant act like a condenser for the back-pressure plant. This means that the back pressure can be lower than the atmospheric pressure. The lower the back pressure the higher the back-pressure plant

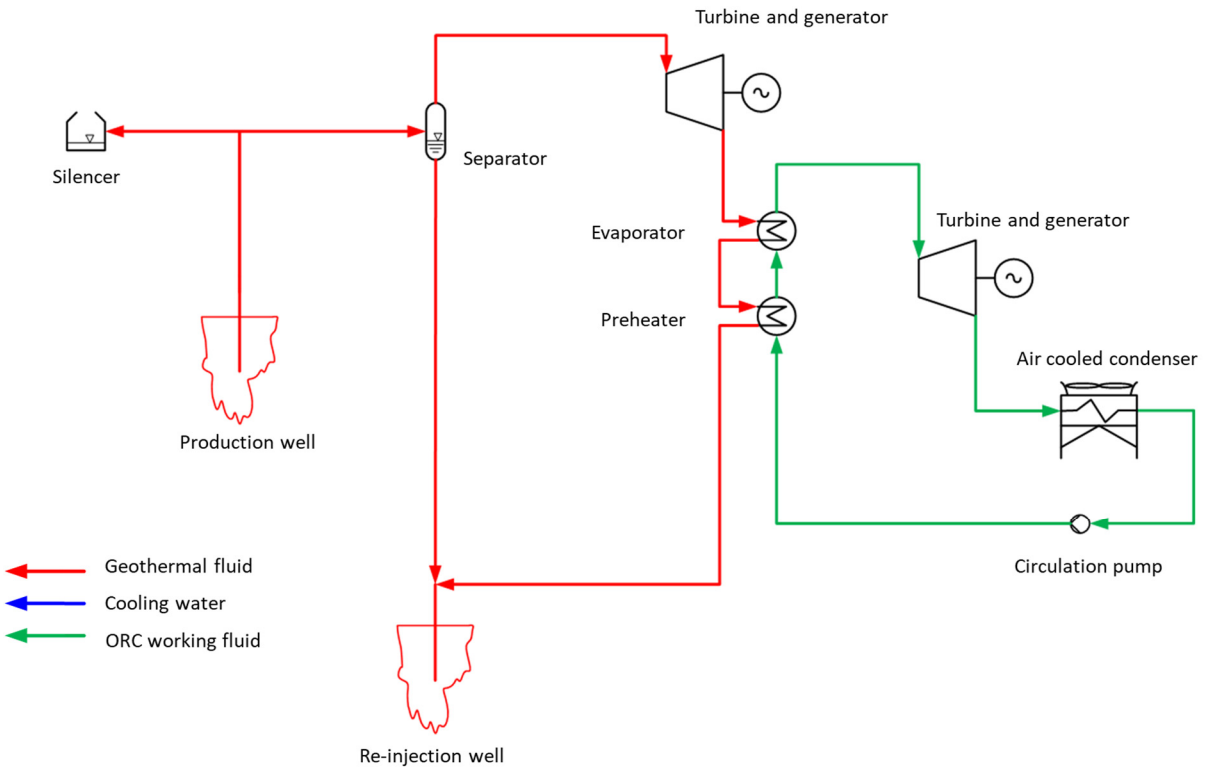

FIGURE 27: Back-pressure plant with an ORC bottoming unit

output and the lower the output for the ORC bottoming plant. A wellhead pressure of 5 bar-g and a separator pressure of 4.5 bar-g is assumed for both wells, allowing for a pressure loss in the collection system and separator.

4.5.1 Well Mon 1

The net power output of the back-pressure plant is shown in Figure 28. The working fluid is selected by comparing the ORC plant output for the different fluids. The steam back-pressure plant power output is the same for all fluids. The ORC power for the studied working fluids is shown in Figure 29. Cyclopentane is the best working fluid in this comparison.

The back pressure will probably be kept at 0 bar-g, at least, in order to avoid a vacuum (Table 18) and the associated air leaks into the cycle. The total net power for well Mon 1 is shown in Figure 30.

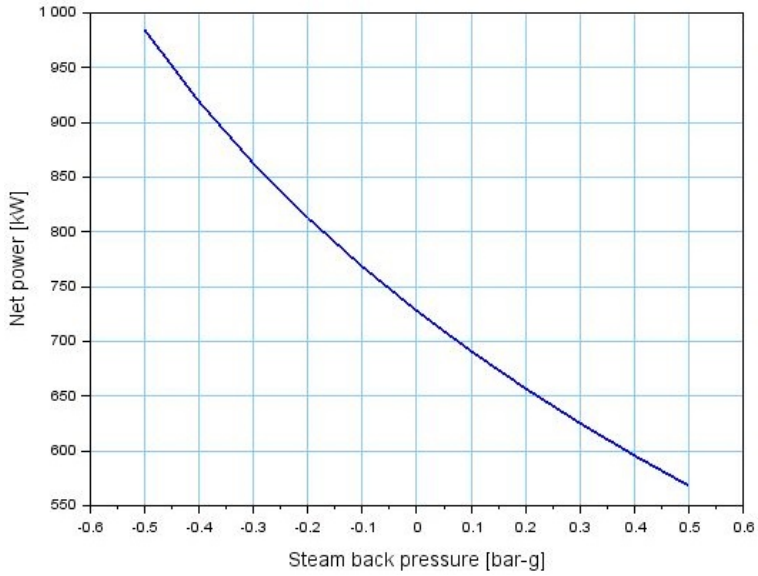

FIGURE 28: Well Mon 1, back-pressure plant power

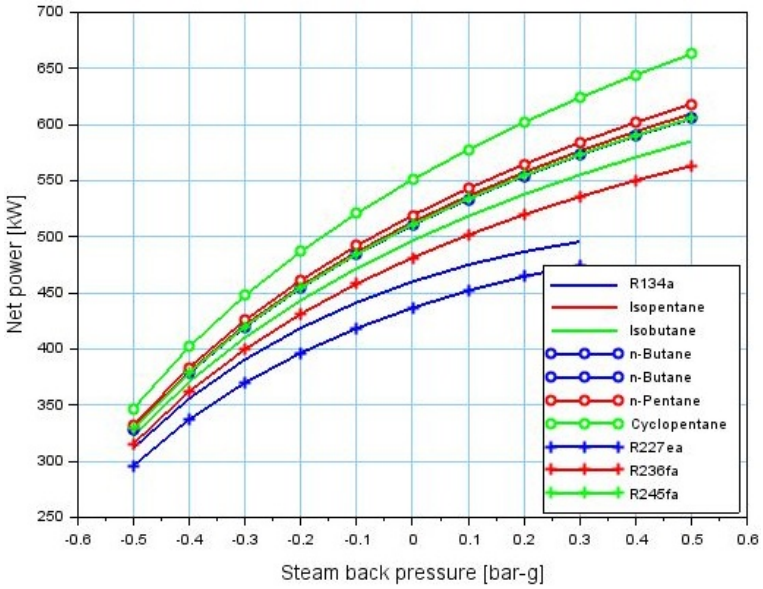

FIGURE 29: Well Mon 1, comparison of ORC working fluids

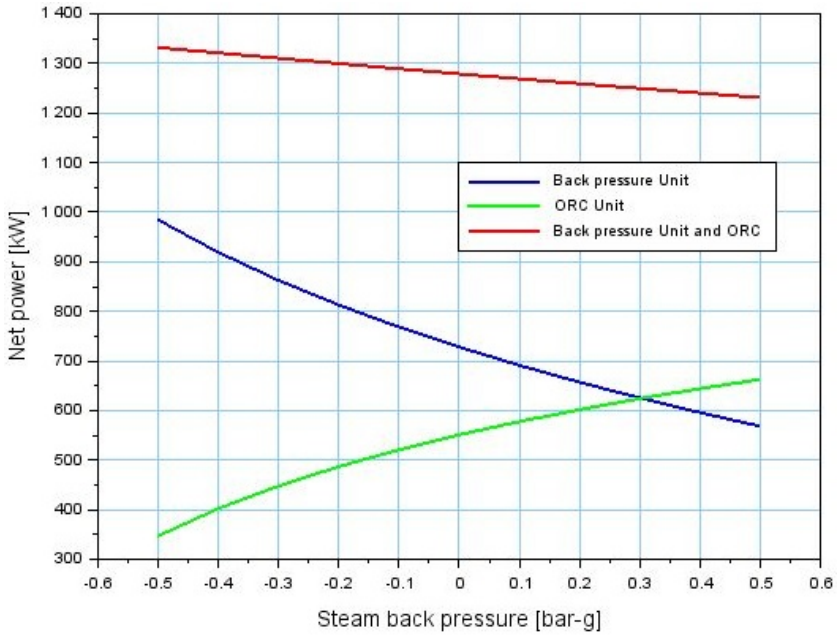

FIGURE 30: Well Mon 1, power output of the back-pressure unit, ORC unit and combination of ORC and back-pressure units

TABLE 18: Mon 1, ORC / back-pressure data

P_BP (bar-g)	W_dot_BP (kW)	W_dot_ORC (kW)	W_dot_total (kW)
-0.5	984.8	347.0	1331.8
-0.4	919.1	402.1	1321.2
-0.3	862.6	447.8	1310.5
-0.2	812.8	486.9	1299.8
-0.1	768.3	520.9	1289.2
0.	727.9	550.9	1278.9
0.1	691.0	577.8	1268.8
0.2	656.9	602.0	1259.0
0.3	625.3	624.1	1249.4
0.4	595.7	644.3	1240.1
0.5	568.0	662.9	1231.0

4.5.2 Well Mon 2

The net power output of the back-pressure plant is shown in Figure 31. The working fluid is selected by comparing the ORC plant output for the different fluids. The steam back-pressure plant power output is the same for all fluids. The ORC power output for the studied working fluids is shown in Figure 32. Cyclopentane is the best working fluid in the comparison.

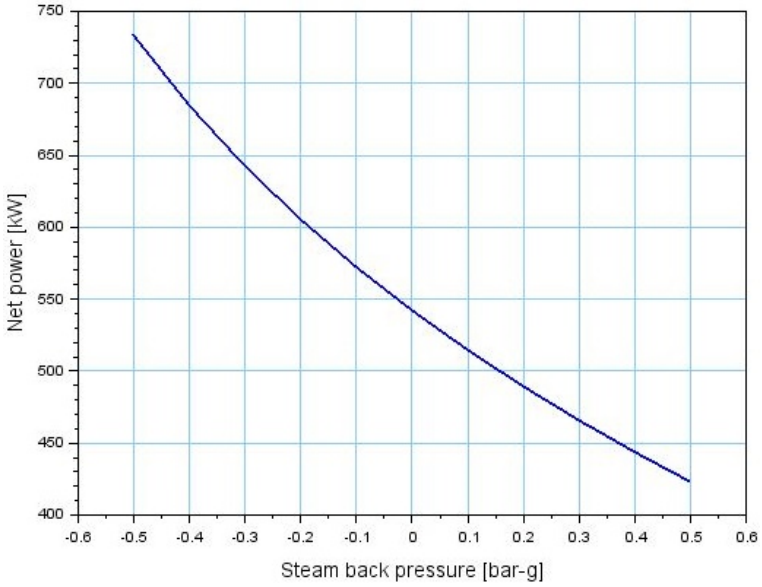

FIGURE 31: Well Mon 2, back-pressure plant power

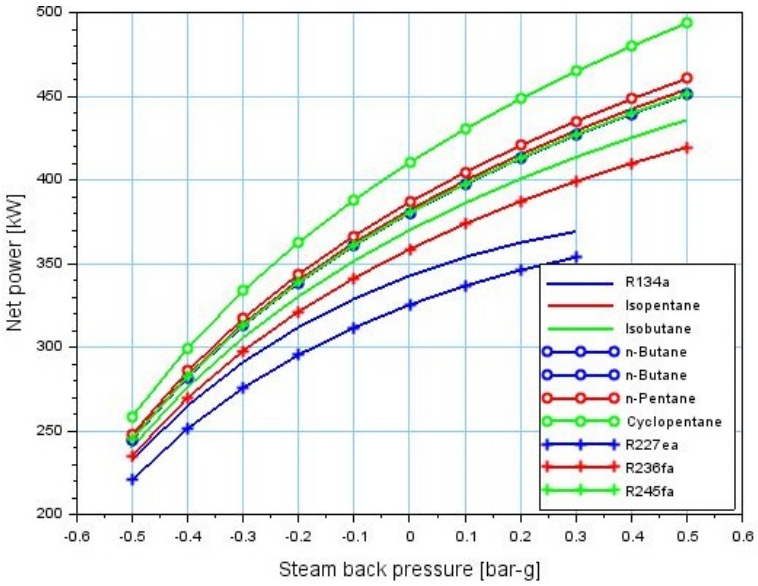

FIGURE 32: Well Mon 2, comparison of ORC working fluids

The back pressure will probably be kept at least at 0 bar-g in order to avoid a vacuum and the associated air leaks into the cycle as shown in Table 19. The total net power for well Mon 2 is shown in Figure 33.

TABLE 19: Mon 2 ORC / back-pressure data

P_BP (bar-g)	W_dot_BP (kW)	W_dot_ORC (kW)	W_dot_total (kW)
-0.5	733.4	258.4	991.8
-0.4	684.5	299.4	984.0
-0.3	642.4	333.5	975.9
-0.2	605.3	362.6	968.0
-0.1	572.1	387.9	960.1
0.	542.1	410.3	952.4
0.1	514.6	430.3	944.9
0.2	489.2	448.3	937.6
0.3	465.7	464.7	930.5
0.4	443.7	479.8	923.5
0.5	423.0	493.7	916.7

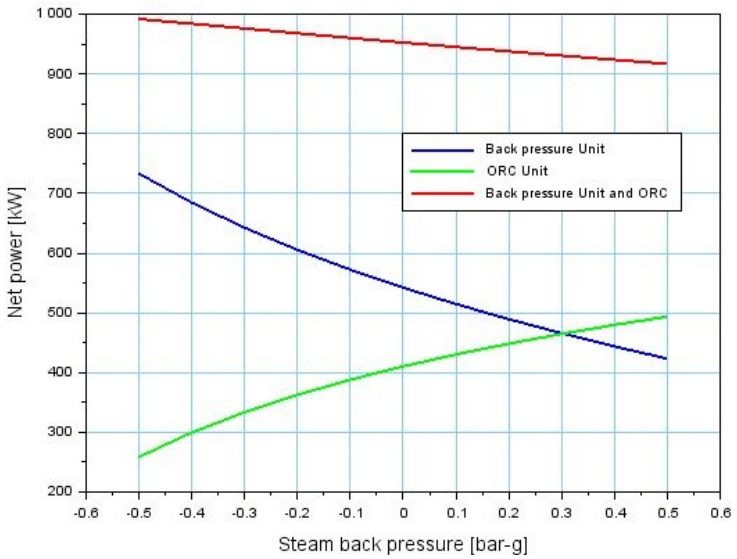

FIGURE 33: Well Mon 2, power output of the back-pressure unit, ORC unit and a combination of ORC and back-pressure units

4.6 Summary of power calculations for all plants

The results of all simulations are summarized in Table 20.

TABLE 20: Power output for all power plants and brine temperature out

	Plants	Total net power (kW)	Brine temperature out (°C)
Mon 1	Single flash	1576.8	136.2
	Binary	1663.8	139.9
	Back pressure	728.7	158.8
	SF bottoming	1888.6	75.0
	thereof ORC	310	75.0
	BP bottoming	1278.9	155.4
	thereof ORC	550.9	99.6
Mon 2	Single flash	1142.9	138.9
	Binary	1188.2	137.4
	Back pressure	546.1	158.8
	SF bottoming	1370.9	74.0
	thereof ORC	228	74.0
	BP bottoming	952.4	155.4
	thereof ORC	542.1	99.6

5. ANALYSIS

In this section the data collected from the simulations using the engineering software Scilab is analysed. First, we compare the single-flash plant to the binary plant for both wells, Mon 1 and Mon 2, then the single-flash to the back-pressure plant and eventually the binary plant to the back-pressure plant.

5.1 Comparisons of power plant types

5.1.1 Single-flash plant – binary plant

First, we compare the single-flash plant to the binary plant. The simulation was run with set variables such as condenser temperature 45°C, enthalpy 973 kg/s, and mass flow 20 kg/s along with data for the Mon 1 well. The power output as a function of the separator pressure with turbine power and net power are shown in Figure 7, it is apparent that the turbine power is much higher than the net power. The data from the simulation of the single-flash plant for Mon 1 is shown in Table 4. The maximum power output of the turbine (1626.3 kW) and the net power (1578.6 kW) at a separator pressure of 2 bar-g and the temperature out is 133.5°C. This is the best turbine and net power output for this plant, but the silica saturation limit is 135°C (Capuano, 2014). Within these limits, the best power turbine and net power output with a temperature above the saturation limit is 1623.3 and 1576.8 kW, respectively, with a separator pressure of 2.25 bar-g and the temperature out is 136.2°C.

For the simulation of the binary power plant, many different secondary fluids were used (highlighted rows in Table 6). This was done because the temperature of the wells (245 and 250°C) are way above the normal range for binary plants which is 85-170°C (Dickson and Fanelli, 2004).

The best turbine and net power output for the binary plant using well Mon 1 are 2239 and 2075 kW, respectively, with a vaporizer pressure of 13.51 bar-g and a temperature out of 93.5°C which is far below the silica saturation limit. The next suitable temperature above the silica limit would be 139.9°C with

turbine and net power of 1801.8 and 1663.8 kW, respectively. This is achieved with the working fluid cyclopentane.

The Mon 2 simulation data for the binary plant is shown in Tables 11-14. Cyclopentane has the highest turbine and net power output of 1569.2 and 1454.2 kW, respectively, with a vaporizer pressure of 13.51 bar-g and a temperature out of 88.8°C. This temperature is also far below the silica saturation limit. The temperature that would satisfy the silica saturation limit is 137.4°C with a turbine power and net power of 1288.4 and 1188.2 kW, respectively, and a vaporizer pressure of 29.23 bar-g. The single-flash plant simulation shown in Figure 10 (with the turbine and net power vs. vaporizer pressure), as shown in Table 5. The turbine and net power output are 1175.7 and 1142.9 kW, respectively, with a separator pressure of 2.5 bar-g and a temperature out of 138.9°C.

5.1.2 Single-flash plant – back-pressure plant

In this section the back-pressure plant is compared to the single-flash plant. The Mon 1 well was analysed with the parameters mentioned above. Figure 7 shows the turbine and net power output as a function of the separator pressure. The best turbine and net power output in Table 4 are 1626.3 and 1578.6, respectively, with a separator pressure of 2 bar-g and a temperature out as 133.5°C. As noted above, the silica saturation limit is 135°C (Capuano, 2014). With this in mind the next best turbine and net power output with a temperature above the saturation limit (highlighted line) is 1623.3 and 1576.8 kW, respectively, with separator pressure at 2.25 bar-g and a temperature out as 136.2°C. For a back-pressure plant at well Mon 1, Figure 25 shows net power as a function of separator pressure. The maximum power output of the wellhead plant is 728.7 kW, with a separator pressure of 5 bar-g and temperature of 158.8°C (highlighted row in Table 16).

The results of the comparison of the back-pressure plant and the single-flash plant for well Mon 2 are shown in Figure 10. As before, Table 4 shows that the turbine and net power of 1626.3 and 1578.6 kW were achieved at a pressure of 2 bar-g with a temperature out of 133.5°C. Considering the silica saturation limit, the turbine and net power are 1623.3 and 1576.8 kW, respectively, with a separator pressure of 2.25 bar-g and a temperature out as 136.2°C. The graph in Figure 26 shows net power as a function of the separator pressure for a back-pressure plant. Table 17 shows the data collected from the simulation and the highlighted row shows the maximum power output of 546.1 kW with a separator pressure of 5 bar-g and a temperature of 158.8°C.

5.1.3 Binary plant – back-pressure plant

In this section the binary plant is compared to the back-pressure plant. The graph in Figure 19 shows the net power as a function of the separator pressure for the back-pressure plant at well Mon 1. Table 16 shows the maximum power output of 728.70 kW, with a separator pressure of 5 bar-g and a temperature out as 158.8°C. For the binary plant at well Mon 1, the best turbine and net power is 2239.0 and 2074.9 kW, respectively, with a vaporizer pressure of 13.51 bar-g and a temperature out as 93.6°C, and was achieved with the working fluid cyclopentane (Table 7). Considering the silica saturation limit, the turbine and net power are 1801.8 and 1663.8 kW, respectively, with a vaporizer pressure of 26.9 bar-g and a temperature out as 139.9°C.

Four secondary fluids were used for the binary plant simulation for well Mon 2. The most suitable was cyclopentane with the highest turbine and net power, 1569.2 and 1454.2 kW, respectively, at a vaporizer pressure of 13.51 bar-g and the temperature out as 88.8°C (Table 11). Considering the silica saturation limit, the turbine and net power are 1288.4 and 1188.2 kW, with a vaporizer pressure of 29.23 bar-g and a temperature of 137.4°C. Figure 26 shows the net power as a function of the separator pressure obtained from the simulation of the back-pressure plant at Mon 2. Table 17 shows the data collected from the simulation. As seen before, the highlighted row shows the maximum turbine and net power of 546.1 kW, with a separator pressure of 5 bar-g and a temperature of 158.8°C.

5.2 The bottoming plant

In this section, the potential of a bottoming plants is analysed. The layout of a single-flash plant with ORC bottoming plant is shown in Figure 21. Table 20 shows the total power output for Mon 1 as 1888.6 kW with a temperature out as 75°C. For Mon 2 the power output is 1370.9 kW and the temperature out is 74°C. The single-flash with ORC bottoming plant shows a very promising power output but the temperature out is far below the silica saturation limit of 135°C. This would cause scaling.

A back-pressure plant with ORC bottoming plant also shows potential and was compared to the other plant types in the report. The layout of a back-pressure with ORC bottoming plant is shown in Figure 27. Figure 29 shows the net power as a function of steam back pressure for Mon 1 for all different working fluids, with cyclopentane achieving the best output. The total combined output of the bottoming plant is 1278.9 kW (Table 18). For well Mon 2 the comparison of the different working fluids is shown in Figure 32. The total combined output for the bottoming plant is 952.4 kW (Table 19). The temperature out for the bottoming plant is not a concern because it uses the steam from the turbine to heat the secondary fluid in the evaporator of the ORC unit and the brine from the separator goes directly to the reinjection reservoir at a temperature of 151.8°C. This temperature is above the silica saturation limit of 135°C.

6. COSTS AND COST ANALYSIS

The first comparison shows that for well Mon 1, the binary plant using cyclopentane as the secondary working fluid produces a 25% higher power output with a higher temperature out than the single-flash plant. Well Mon 2 has a 23% higher output using the binary plant rather than the single-flash plant. The second comparison shows that for well Mon 1 the single-flash plant produces 73.6% more power output than the back-pressure plant. For well Mon 2, this comparison shows 70.6% more power from the single-flash power plant. For Mon 1, the binary plant has 95% increased power output compared to the back-pressure plant. Well Mon 2 shows almost the same increase in power output, or 90.8%. Using a single-flash bottoming plant, well Mon 1 has a 31.7% higher power output than well Mon 2. For the back-pressure bottoming plant, Mon 1 has a 29.3% higher power output than well Mon 2.

Analysing all three comparisons shows that a binary plant using cyclopentane as secondary fluid is the best option for both wells. The single-flash plant yields good results, too. The back-pressure plants, however, did not produce much power because of the pressure limitation. The bottoming plants have potential but are limited by the scaling, which might occur.

6.1 Cost analysis

According to Hance (2005), very few cost estimates have been published. Therefore, we need to rely on information from geothermal plant component manufacturers and installers. Geothermal energy production is one of few technologies with near zero fuel costs. This, combined with a high capacity factor, means that geothermal heat is one of the most reliable energy sources available today (Alyssa, 2006).

6.1.1 The power plant

As stated by DiPippo (1999), the cost associated with building and operating a geothermal power plant fluctuates widely and depends on factors such as:

- Resource type:
- Resource temperature;
- Reservoir productivity;

- Power plant size (rating);
- Power plant type;
- Environmental regulations;
- Cost of capital;
- Cost of labour.

The cost for a geothermal plant is very site specific. Below are the factors which were used in the simulation to calculate cost and size of the power plants:

- ✓ Heat transfer coefficients (U) (Ahangar, 2012);
- ✓ U evaporator = 1000 W/m^2 °C;
- ✓ U pre-heater = 600 W/m^2 °C;
- ✓ U air-cooled condenser = 500 W/m^2 °C;
- ✓ U steam condenser = 2000 W/m^2°C;
- ✓ Plant lifespan = 30 years;
- ✓ Discount rate = 15%;
- ✓ Operation and maintenance cost = 4% of gross income;
- ✓ Cost of steam gathering system = 280 USD/kW (Hance, 2005);
- ✓ Electricity tariff = 0.20 USD/kWh (Zuliani and McKee, 2019);
- ✓ Plant components unit cost (UC) (Ahangar, 2012) – revised;
- ✓ UC vaporizer = 300 USD/m^2;
- ✓ UC pre-heater = 300 USD/m^2;
- ✓ UC air-cooled condenser = 400 USD/m^2;
- ✓ UC steam condenser = 300 USD/m^2;
- ✓ UC turbine = 600 USD/kW;
- ✓ UC pump = 600 USD/kW;
- ✓ The cost for the plant systems, that is engineering and construction, balance of plant, and BOP, are assumed to be the same as the purchased equipment cost (PEC). In the case of the back-pressure plant this cost is assumed to be 120% of the PEC.

Table 21 shows the cost for components and the entire plant for a single-flash plant using well Mon 1 as well as well Mon 2. Table 22 shows the cost for components and the entire plant for a binary plant. Table 23 shows the cost for a single-flash plant with bottoming ORC. Table 24 shows the cost for a back-pressure plant. Finally, Table 25 shows the cost for the back-pressure plant with ORC bottoming plant.

TABLE 21: Cost for a single-flash plant

	Component	Size	Unit	Cost (USD)
Mon 1 single flash	TurboGenerator	1626	kW	975,834
	Condenser	275	m^2	82,607
	Cooling tower	8381	kW	167,633
	Purchased equipment cost (PEC)	-	-	1,226,075
	Cost of balance of plant (BOP)	100	%	1,226,075
	Total plant cost	-	-	2,452,151
	Net power specific cost?*	1578	kW	1,553
Mon 2 single flash	TurboGenerator	1176	kW	705,452
	Condenser	189	m^2	56,804
	Cooling tower	5764	kW	115,272
	Purchased equipment cost (PEC)	-	-	877,529
	Cost of balance of plant (BOP)	100	%	877,529
	Total plant cost	-	-	1,755,059
	Net power specific cost*	1143	kW	1,535

* Investment cost per kW net power

TABLE 22: Cost for an ORC plant

	Component	Size	Unit	Cost (USD)
Mon 1 ORC	TurboGenerator	1626	kW	1,343,430
	Air cooled condenser	1420	m^2	567,856
	Vaporizer	242	m^2	72,845
	Preheater	526	m^2	157,671
	Circulation pump	45	kW	27,167
	Purchased equipment cost (PEC)			2,168,971
	Cost of balance of plant (BOP)	100	%	2,168,971
	Total plant cost	-	-	4,337,943
	Net power specific cost	2074	kW	2090
Mon 2 ORC	TurboGenerator	1569	kW	941,575
	Air cooled condenser	994	m^2	397,995
	Vaporizer	164	m^2	49,201
	Preheater	397	m^2	119,100
	Circulation pump	31	kW	19,041
	Purchased equipment cost (PEC)	-	-	152,6915
	Cost of balance of plant (BOP)	100	%	152,6915
	Total plant cost	-	-	3,053,830
	Net power specific cost	1454	kW	2099

TABLE 23: Cost of a bottoming ORC plant added to the single-flash plant in Table 25

	Component	Size	Unit	Cost (USD)
Mon 1 ORC + bottoming for single flash	TurboGenerator	375	kW	225,228
	Air cooled condenser	495	m^2	197,821
	Vaporizer	146	m^2	43,810
	Preheater	189	m^2	56,856
	Circulation pump	24	kW	14,530
	Purchased equipment cost (PEC)	-	-	538,246
	Cost of balance of plant (BOP)	100	%	538,246
	Total plant cost	-	-	1,076,492
	Net power specific cost	310	kW	3475
Mon 2 ORC + bottoming for single flash	TurboGenerator	276	kW	165,367
	Air cooled condenser	346	m^2	138,331
	Vaporizer	96	m^2	28,746
	Preheater	147	m^2	44,211
	Circulation pump	18	kW	11,187
	Purchased equipment cost (PEC)	-	-	387,841
	Cost of balance of plant (BOP)	100	%	387,841
	Total plant cost	-	-	775,682
	Net power specific cost	1143	kW	3402

TABLE 24: Cost for a back-pressure plant

	Component	Size	Unit	Cost (USD)
Mon 1 back pressure	TurboGenerator	729	kW	437,274
	Purchased equipment cost (PEC)	-	-	437,274
	Cost of balance of plant (BOP)	120	%	524,729
	Total plant cost	-	-	962,003
	Net power specific cost	729	kW	1320
Mon 2 back pressure	TurboGenerator	546	kW	327,719
	Purchased Equipment Cost (PEC)	-	-	327,719
	Cost of Balance of Plant (BOP)	120	%	393,263
	Total plant cost	-	-	720,983
	Net power specific cost	546	kW	1320

TABLE 25: Cost for a bottoming ORC plant added to the back-pressure plant in Table 28

	Components	Size	Unit	Cost (USD)
Mon 1 ORC bottoming for back pressure	TurboGenerator	622	kW	373,206
	Air cooled condenser	786	m^2	314,462
	Vaporizer	771	m^2	231,411
	Preheater	89	m^2	26,710
	Circulation pump	5.25	kW	3,152
	Purchased equipment cost (PEC)	-	-	948,941
	Cost of balance of plant (BOP)	100	%	948,941
	Total plant cost	-	-	1,897,883
	Net power specific cost	551	kW	3445
Mon 2 ORC bottoming for back pressure	TurboGenerator	463	kW	277,818
	Air cooled condenser	585	m^2	234,088
	Vaporizer	574	m^2	172,264
	Preheater	66	m^2	19,883
	Circulation pump	3.96	kW	2,346
	Purchased equipment cost (PEC)	-	-	706,400
	Cost of balance of plant (BOP)	100	%	706,400
	Total plant cost	-	-	1,412,799
	Net power specific cost	410	kW	3445

6.1.2 Cost of operation and maintenance

Operation and maintenance cost for a geothermal plant varies from plant to plant due to the environment, chemical composition of the fluid and many other factors. Here, a total O&M cost of 3% of the investment is assumed for the steam and flash plants and 4% for the ORC plants.

6.1.3 Cost of steam gathering system

The steam gathering system is the network of pipes connecting the power plant with all production and injection wells. The cost for these facilities varies widely depending on the distance from the production and injection wells to the power plant, the flow pressure and chemical composition of the produced fluids. Carbon steel pipelines are used in the majority of geothermal fields and can be installed completely for USD 15-25 per inch of diameter per foot of pipe length. For highly corrosive brine, alloy systems such as various duplex stainless, high nickel alloys or lined pipes can be 2 to >5 times the cost of carbon steel. For the cost estimate, the initial cost of 250 USD/kW is used (Hance, 2005), corrected with an inflation rate of 2.2% per year, it is 280 USD/kW.

The steam gathering system is assumed to be the same for all plant types. The cost estimate of 280 USD/kW is based on a single-flash plant, and therefore the steam gathering system cost estimate is based on the net power of the single-flash plant as described in Sections 4.1.1 and 4.1.2. The steam gathering system cost estimated for well Mon 1 is thus based on a net power of 1578 kW, and for well Mon 2 1143 kW, resulting in a cost of USD 441,840 for well Mon 1 and USD 320,003 for well Mon 2.

The investment cost estimate as well as an estimate of the yearly energy production assuming 7500 hours production per year is shown in Table 26.

TABLE 26: Power output for all power plants and total investment cost

	Plant type	Total net power (kW)	Yearly energy (GWh)	Plant cost (USD)	Steam system cost (USD)	Total investment (USD)
Mon 1	Single flash	1,579	11.84	2,452,151	441,840	2,893,991
	Binary	2,048	15.36	4,337,943	441,840	4,779,783
	Back pressure	729	5.46	962,003	441,840	1,403,843
	SF bottoming ORC	310	2.32	1,076,492	0	1,076,492
	BP bottoming ORC	551	4.13	1,897,883	0	1,897,883
Mon 2	Single flash	1,143	8.57	1,755,059	320,003	2,075,062
	Binary	1,454	10.90	3,053,830	320,003	3,373,833
	Back pressure	546	4.09	720,983	320,003	1,040,986
	SF bottoming ORC	228	1.71	775,6820	0	775,682
	BP bottoming ORC	542	4.06	1,412,799	0	1,412,799

The wells are not included in this investment cost estimate. They do already exist and are considered sunk cost.

Now an estimate of the yearly cost of the plants and of the cost of electricity production can be made (Table 27).

TABLE 27: Yearly cost and estimate of the cost of electricity

	Plant type	Yearly capital cost, discount 15% (USD)	Depreciation 30 years (USD)	O&M cost 3 or 4% (USD)	Total yearly cost (USD)	Cost of electricity (USD/kWh)
Mon 1	Single flash	374,450	82,379	74,890	531,719	0.045
	Binary	657,319	144,610	175,285	977,214	0.064
	Back pressure	150,928	33,204	30,186	214,318	0.039
	SF bottoming ORC	161,474	35,524	43,060	240,058	0.103
	BP bottoming ORC	284,682	62,630	75,915	423,228	0.102
Mon 2	Single flash	311,259	68,477	62,252	441,988	0.052
	Binary	506,075	111,336	134,953	752,365	0.069
	Back pressure	156,148	34,353	31,230	221,730	0.054
	SF bottoming ORC	116,352	25,598	31,027	172,977	0.101
	BP bottoming ORC	211,920	46,622	56,512	315,054	0.078

6.2 Revenue estimation

Additional to the cost estimation, it is imperative to calculate an estimate of the revenues from each of the different plant types. In order to do this calculation, the power output results are converted into the energy that is produced during a one-year period using the assessed capacity factor (Hance 2005).

$$\frac{revenue}{year} = net\ power\ output * 365 * 24 * c.f * price \quad (3)$$

The revenue estimation in this report is based on the power output from the simulations and cost of electricity which is 0.20 USD/kW (Zuliani and McKee, 2019). The capacity factor used is 90% (Cordova et al., 2013). Only the best two plant types are used for revenue estimation, i.e. the binary plant and the single-flash plant for well Mon 1. Costs shown in Table 28 are rough estimates using Equation 3.

TABLE 28: Revenue estimate for feasible Montserrat power plants

Plant type	Power output (kW)	Revenue / year (USD)
Single flash	1,579	2,489,136
Binary	2,048	3,229,129

7. RECOMMENDATIONS AND CONCLUSIONS

In this project three different types of power plants, namely single-flash, binary and back-pressure plants, were compared using two wells Mon 1 and Mon 2. Recommendations are listed below:

- Mon 1 should be used for power production because it has a better overall power output with all three plant types.
- The drilling of an injection well and the use of both Mon 1 and Mon 2 as production wells would increase the power production.
- The removal of the small diameter liner from well Mon 2 would increase the mass flow which would then increase the power output of the well.
- The binary plant would be most efficient, followed by the single-flash power plant for the harnessing of geothermal energy. A back-pressure plant is the least favourable due to its low power output but it has the lowest cost per kWh.
- Using geothermal energy for electricity production would stabilize the grid and reduce the dependence on fossil fuels with uninterrupted base load power.
- To finance the plant construction a joint approach including local financial institutions, funding partners and agencies is desirable.

Geothermal energy is one of the leading sources of energy to meet the increased demand for clean energy. This project concludes that the binary plant is the best option from the power output perspective, with cyclopentane as the secondary fluid. As seen from the simulation, the binary plant has the highest power output compared to the other plant types (Table 26). The yearly cost for running this plant and its estimated electricity cost, however, are much higher than for the others types (Table 27).

Although the investment cost for the binary plant is higher than for the other plants, it produces much more power. The cost for producing electricity is around 0.064 to 0.069 USD/kWh. The total yearly cost for running the plant is around USD 977,214 without fossil fuel cost. This initiative would significantly reduce the island's importation and dependence on fossil fuels.

The development of a binary plant on the island of Montserrat would create many opportunities. It would reduce the fossil fuel consumption for the island, reduce green-house gas emission and subsequently the island's carbon footprint. A thermal spa and wellness facilities utilizing geothermal energy would boost the local tourist industry and create business opportunities for the local population. The drying of agriculture products such as fruits and grains as well as the drying of fish stock and cold storage are other benefits that could be derived from the construction and operation of a geothermal plant.

Electricity prices would drop, having a positive impact on household spending, leaving residents with more disposable income.

In conclusion, based on the evidence presented in this study, the Government of Montserrat should invest in a binary geothermal plant to improve the livelihood of its citizens.

ACKNOWLEDGEMENTS

I would like to thank Mr Lúdvík S. Georgsson for the invitation to attend the UNU six months training programme, also the supporting staff Ingimar, Frída, Markús, Vigdís and Thórhildur. This work would never have been accomplished if it were not for the help and support I received from my supervisors, Dr. Páll Valdimarsson and Dr. María Sigrídur Gudjónsdóttir.

Thanks to the Permanent Secretary, Mrs. Beverley Mendes, and Managing Director of MUL, Mr Kendall Lee, for allowing me to attend this training. I would like to especially thank my wife, Lavern, and our two beautiful daughters, Keilah and Kearah, for their patience, understanding and support over the past six months.

I would like to thank God the almighty for sparing my life to attend this six-months training and also for travelling mercies.

NOMENCLATURE

A	= Area (m²);
C.f.	= Capacity factor;
Net power output	= Gross power output – parasitic load;
Price	= In this project USD/kWh is used for the price of electricity;
T	= Temperature (C).

REFERENCES

Ahangar, F.A., 2012: Feasibility study of developing a binary power plant in the low-temperature geothermal field in Puga, Jammu and Kashmir, India. Report 6 in: *Geothermal training in Iceland 2011.* UNU-GTP, Iceland, 1-24.

Alyssa, K., 2006: *A handbook on the externalities, employment, and economics of geothermal energy*. Geothermal Energy Association, Washington, DC, 75 pp.

Battocletti, L., 1999: *Geothermal resources in Latin America and the Caribbean*. Bob Lawrence and Associates, Inc., for Sandia National Laboratories, Contract No. AS-0989, 214 pp.

Brophy, P., Suemnicht, G., Poux, B., Hirtz, P., and Ryan, G., 2014: Preliminary results of deep geothermal drilling and testing on the Island of Montserrat. *Proceedings of the 39th Workshop on Geothermal Reservoir Engineering, Stanford University, Stanford, CA,* 11 pp.

Capuano, 2014: *Montserrat geothermal wells long term test report (final report)*. Government of Montserrat, Capuano Engineering Company, CA, report, 173 pp.

Clark, J.G., 2014: *Optimal design of geothermal power plants*. Virginia Commonwealth University, Richmond, Virginia, 204 pp.

Cordova Geirdal, C.A., Gudjónsdóttir, M.S., Jensson, P., 2013: Economic comparison between a well-head geothermal power plant and a traditional geothermal power plant. *Proceedings of the 38th Workshop on Geothermal Reservoir Engineering, Stanford University, Stanford, CA,* 9 pp.

Dickson M.H., and Fanelli, M., 2004: *What is geothermal energy*? Instituto di Geoscienze e Georisorse, CNR, Pisa, 61 pp.

DiPippo, R, 1999: *Small geothermal power plant: design, performance and economics*. University of Massachusetts, Dartmouth, MA, Mechanical Engineering Department, GHC Bulletin, June, 8 pp.

DiPippo, R., 2015: *Geothermal power plants*. *Principles, applications, case studies and environmental impac*t (4th ed.). Butterworth-Heinemann, 800 pp.

Gudmundsson, Y., and Hallgrímsdóttir, E., 2016: Wellhead power plants. *Proceedings of the 6th African Rift Geothermal Conference ARGeo-6, Addis Ababa,* 9 pp.

Hance, C.N., 2005: *Factors affecting costs of geothermal power development*. Geothermal Energy Association for the US Department of Energy, August, 64 pp.

MCWL&E, 2016: *The power to change, Montserrat energy policy 2016-2030.* Government of Montserrat, W.I., website:
www.gov.ms/wp-content/uploads/2016/02/The-Power-to-Change-MNEP-Cabinet-Approved.pdf

Petrowicki, 2019: *Production forecasting decline curve analysis*. Petrowiki, website:
petrowiki.org/Production_forecasting_decline_curve_analysis

Sanyal, S.K., Menzies, A.J., Brown, P.J., Enedy, K.L., and Enedy, S., 1989: A systematic approach to decline curve analysis for The Geysers steam field, California. *Geothermal Resources Council, Transactions, 13*, 415-421.

Sanyal, S.K., Butler, S.J., Brown, P.J., Goyal, K., and Box, T., 2000: An investigation of productivity and pressure decline trends in geothermal steam reservoirs. *Proceedings of the World Geothermal Congress 2000, Kyushu - Tohoku, Japan*, 5 pp.

Valdimarsson, P., 2011: Geothermal power plant cycles and main components. *Papers presented at "Short Course on Geothermal Drilling, Resource Development and Power Plants", organized by UNU-GTP and LaGeo, in Santa Tecla, El Salvador,* UNU-GTP SC-12, 24 pp.

Worldometer, 2019: *Montserrat electricity.* Worldometer, website:
www.worldometers.info/electricity/montserrat-electricity/

Zuliani, J., and McKee, K., 2019: *Integrated resource plan, cost of service and tariff study.* Montserrat Utilities Ltd., HATCH, 111 pp.